ELSEVIER

Chemical Geology 204 (2004) 63–102

CHEMICAL GEOLOGY
INCLUDING
ISOTOPE GEOSCIENCE

www.elsevier.com/locate/chemgeo

Rare earth element evolution of Phanerozoic seawater recorded in biogenic apatites

Christophe Lécuyer[a,*], Bruno Reynard[b], Patricia Grandjean[c]

[a] *Laboratoire CNRS UMR 5125 Paléoenvironnements and Paléobiosphère, Université Claude Bernard Lyon 1, Campus de la Doua, F-69622 Villeurbanne, France*

[b] *Laboratoire de Sciences de la Terre, CNRS UMR 5570, Ecole Normale Supérieure de Lyon, 46 Allée d'Italie, F-69364 Lyon, France*

[c] *8 Avenue Roberto Rossellini, 69100 Villeurbanne, France*

Accepted 8 November 2003

Abstract

Rare earth element (REE) contents of marine biogenic apatites have been shown to record seawater compositions. A data base of available and newly acquired rare earth element (REE) contents of marine biogenic apatites has been created to assess the past seawater REE compositions. To ensure that this data base contains only the pristine REE signals, altered samples, characterized by very low $(La/Sm)_N$ ratios (where N stands for REE ratios normalized to the NASC composition; Gromet et al., 1984, Geochim. Cosmochim. Acta 48 (1984) 2469) acquired during apatite recrystallization, are not included in the database. These data reveal a change in the Tethyan seawater composition between 110 and 80 Ma. After the end of the Cretaceous, the REE chemistry of seawater remains constant until present-day. This seawater composition change is likely due to concurrent changes in REE scavenging processes. A strong correlation between decreasing $(Sm/Yb)_N$ ratios and increasing Ce anomalies for samples deposited during the 80–110 Ma period is observed. As Ce anomalies are attributed to ocean water redox conditions, changes in REE scavenging could reflect an evolution from stratified and poorly oxygenated waters towards well-mixed and oxygenated waters. This could have resulted from changing current patterns stemming from the contemporaneous opening of the Atlantic Ocean. A major change in Middle and Late Cretaceous oceanic circulation linked to plate tectonics would have favored the colonization of pelagic environments.

Keywords: Rare earth element; Phanerozoic; Biogenic apatites

1. Introduction

Biogenic phosphates may trace the chemistry of ancient seawater because the rare earth elements (REE) spectra of modern marine remains mimic those of surrounding seawater (Elderfield and Pagett, 1986; Grandjean et al., 1987). Enrichment factors of 10^6–10^7 relative to seawater result from pre-concentration processes by primary carriers in the water column (Bernat, 1975). Primary carriers of REE from near-surface waters to the sea floor are both inorganic like metal hydroxides and organic particles such as zooplankton and fecal pellets (Boyle et al.,

* Corresponding author. Also at Institut Universitaire de France, 103 Boulevard Saint-Michel, 75005 Paris, France. Fax: +33-7243-1688.

E-mail address: clecuyer@univ-lyon1.fr (C. Lécuyer).

0009-2541/$ - see front matter © 2003 Elsevier B.V. All rights reserved.
doi:10.1016/j.chemgeo.2003.11.003

1977; Aplin, 1984; Fowler et al., 1987). REE are released by organic material during its oxidation within the water column, especially at the water–sediment interface, and are adsorbed by apatite in the sediments during early diagenesis (Grandjean et al., 1987) without significant REE fractionation (Koeppenkastrop and De Carlo, 1992; Koeppenkastrop et al., 1991). The preservation of this paleoceanographic signal in marine vertebrate remains depends on the extent of REE addition and fractionation during post-depositional recrystallization ("extensive diagenesis") (Reynard et al., 1999). This diagenetic effect is characterized by a strong middle REE (MREE) enrichment relative to LREE and HREE, leading to "bell-shaped" patterns, as defined by Lécuyer et al. (1998). Taking into account the occurrence of such alteration processes that may distort the original geochemical record, we here investigate the evolution of REE contents of marine biogenic phosphates throughout the Phanerozoic in relation to potential major changes in chemistry and oceanography of Tethyan–Atlantic marine platform domains. We deliberately focus this investigation on biogenic remains and exclude massive phosphorite whose formation conditions are less understood and may not reflect the seawater composition even in contemporary unaltered deposits (e.g. Elderfield and Sholkovitz, 1987).

2. Samples and methods

REE compositions of about 400 samples have been compiled from the literature (data base and references available as electronic supplement). The sampling covers various marine platforms since the Cambrian, but the Mesozoic fish remains mainly come from Tethyan continental shelves. Thirty-one REE analyses were obtained by inductively coupled plasma and mass spectrometry (ICP-MS) at the Ecole Normale Supérieure of Lyon on Cretaceous fish teeth from Western Europe. The samples have been carefully selected from limestones deposited in offshore environments (for precise sample description and location, see Pucéat et al., 2003). Fish teeth were rinsed twice in tridistilled water and etched in 0.2 ml nitric acid 10 N. Only solutions with no apparent residue have been kept for REE analysis; 0.1 ml of a 1 ppm In and Bi internal standard solution was added and the volume taken to a final 5 ml, which is the approximate sample consumption for three trace element analysis runs. Calibration curves were generated against the BHV01 basalt standard provided by the USGS. Addition of In and Bi spikes to the samples was used to correct the beam intensity for ionisation suppression. Series were made of two solutions of known concentrations, one standard rock, three blanks, and 10 samples. Analyzed mass counts were then normalized with respect to the appropriate internal standard intensity.

3. Results

Both literature data and new measurements (Tables 1 and 2) of REE contents in marine biogenic apatites from shoreface to offshore sediments provide a database for deciphering the potential evolution of seawater REE chemistry throughout the Phanerozoic. Three main types of REE patterns are found (Fig. 1). Firstly, samples younger than 80 Ma display patterns similar to those of present-day seawaters. Secondly, samples older than 110 Ma display REE patterns with a relative depletion in HREE and weak Ce anomalies. Samples between 110 and 80 Ma show a progressive evolution between these two types. Thirdly, some samples are characterized by a relatively strong MREE enrichment typical of previously defined "bell-shaped" REE patterns. These patterns have been shown to result from extensive recrystallization during diagenetic alteration, which overprints the pristine composition (Reynard et al., 1999). We therefore removed from the database samples with lowest $(La/Sm)_N$ ratios (Fig. 2). The chosen criterion was to eliminate data with $(La/Sm)_N$ ratios lower than 0.3 (Reynard et al., 1999). Most of these samples are also characterized by low $\delta^{18}O$ values (< 18 ‰) which suggest alteration by non-marine diagenetic fluids (Lécuyer et al., 1998).

Among remaining patterns, the most striking difference is that the oldest samples are depleted in HREE relative to LREE, while samples younger than the late Cretaceous are characterized by the LREE depletion typical of modern seawater. To illustrate this evolution, we have plotted the temporal evolution of

Table 1
Stratigraphic age, location, depositional environments and REE contents of Cretaceous fish teeth from the western Tethyan domain

Samples	Location	Taxon	Lithology	Environment	Age (Ma)	La (ppm)	Sm (ppm)	Yb (ppm)	ΣREE	$(La/Sm)_N$	$(Sm/Yb)_N$	Ω (Ce)
PC21	Puchevillers, France	undetermined fish	limestone	platform	82.1	3.50	0.23	0.20	3.92	2.21	0.60	– 0.64
H2	Malakoff, France	undetermined fish	limestone	platform	73.8	25.11	6.41	1.64	33.16	0.57	1.99	– 0.08
M3	Hallencourt, France	*Scapanorhynchus* sp.	limestone	offshore	82.1	0.92	0.06	0.04	1.02	2.20	0.77	– 0.59
D10	Sens, France	*Squalicorax pristodontus*	limestone	offshore	82.1	21.59	1.42	1.46	24.47	2.20	0.50	– 0.64
PI27	Somme, France	undetermined fish	limestone	upper offshore	87.4	11.03	1.18	0.31	12.52	1.36	1.92	– 0.63
D12	Beauval, France	undetermined fish	limestone	upper offshore	77.4	0.41	0.03	0.04	0.48	1.86	0.44	– 0.53
H6	Authon, France	undetermined fish	limestone	offshore	84.6	157.41	62.51	10.71	230.63	0.37	2.97	– 0.30
M2	Le Mans, France	*Squalicorax falcatus*	shales	upper offshore	94.5	14.28	1.66	0.56	16.49	1.25	1.51	– 0.085
PI23	Ardèche, France	undetermined fish	sandy limestone	upper offshore	91.2	40.35	6.87	1.79	49.01	0.85	1.95	0.055
M1	Les Renardières, France	*Carcharias amonensis*	sandy shales	upper offshore	94.5	7.59	2.10	0.42	10.11	0.53	2.55	0.05
D9	Yonne, France	*Lamna acuminata*	limestone	upper offshore	97.4	35.71	5.63	2.00	43.34	0.92	1.43	– 0.24
D5	Ardennes, France	*Odontaspis* sp.	green clays, phosphates	platform	105.5	25.15	5.90	2.23	33.28	0.62	1.35	0.50
D7	Courcelles, France	Lamniform	shales	upper offshore	105.6	262.72	51.48	5.49	319.69	0.74	4.77	– 0.09
PS25	La Houpette, France	*Otodus* sp.	sands, phosphorites	upper offshore	105.5	106.90	14.85	1.80	123.55	1.05	4.19	0.71
D2	Ardèche, France	*Otodus* sp.	shales	offshore	114.7	30.79	2.57	0.92	34.29	1.74	1.42	0.52
D3	Ardèche, France	*Pycnodus* sp.	shales	offshore	114.7	18.73	5.52	1.53	25.79	0.49	1.83	0.16
PI31	Ain, France	undetermined fish	limestone	platform	105.5	70.95	11.16	2.90	85.01	0.92	1.95	0.03
PI26	Viry, France	undetermined fish	unknown	shoreface	105.5	77.77	12.05	4.50	94.32	0.94	1.36	0.07
D4	Grusse, France	Lamniform	sandstone	shoreface	109.3		6.93	5.63	12.66		0.63	
D6	Bellegarde, France	*Odontaspididae gracilis*	shales	upper offshore	120	79.27	14.07	5.26	98.61	0.82	1.36	0.04
D13	Martigues, France	undetermined fish	limestone	lower offshore	116.1	90.99	9.44	6.88	107.30	1.40	0.70	0.08
D1	Yonne, France	*Sphaerodus neocomiensis*	sandy limestone	upper offshore	129.5	16.81	2.76	1.14	20.71	0.89	1.22	0.17
V42	Auberson, Suisse	undetermined fish	limestone	upper offshore	134.8	255.18	91.91	10.02	357.11	0.40	4.66	0.30
V40	Bonvillars, Suisse	undetermined fish	limestone	offshore	137.5	94.66	33.20	3.78	131.64	0.41	4.46	1.21
V39	Ponte du Suchet, Suisse	undetermined fish	unknown	platform	136.2	396.39	175.97	11.17	583.53	0.33	8.00	0.17
G2	Val de Fier, France	*Pycnodus* sp.	limestone	upper offshore	137	53.68	23.19	1.26	78.13	0.34	9.36	0.49
VSR	Gard, France	undetermined fish	limestone	offshore	136.75	6.43	22.50	1.26	30.18	0.04	9.09	0.21
G1	Ardèche, France	undetermined fish	shales	offshore	138.5	43.40	135.79	7.27	186.46	0.05	9.49	0.22
M4	Texas, USA	undetermined fish	unknown	platform	96.2	108.58	13.45	3.52	125.55	1.17	1.94	0.04
M5	Agadir, Morocco	*Squalicorax falcatus*	limestone	platform	91.25	44.29	4.40	1.68	50.36	1.46	1.33	– 0.30
M6	Texas, USA	undetermined fish	unknown	platform	88.5	72.01	6.46	5.40	83.87	1.62	0.61	– 0.11

Table 2
Stratigraphic age, location, depositional environments and REE contents of Phanerozoic marine biogenic apatites

Samples	Location	Taxon	Material	Lithology	Environment	Period/stage	Proposed age (Ma)	La (ppm)	Ce (ppm)
Grandjean et al. (1987)									
P1	Cevennes, France	*Hybodus*	tooth	sandstone	neritic	Trias	215	65	176
P3	Oman	*Asteracanthus*	tooth	sandstone	neritic	Upper Jurassic	150	259	165.3
P4	Boulonnais, France	*Sphenodus*	tooth	clay	littoral	Portlandian	145	544	672
P5	Vaucluse, France	*Protolamna*	tooth	clay	littoral	Upper Aptian	108	471	11.135
P7	Texas, USA	*Cretolamna*	tooth	sandstone	neritic	Albian	103	243	600
P8	Angola	*Cretolamna*	tooth	sandstone/ clay	neritic	Cenomanian	98	719	1007
P9	Agadir, Morocco	*Cretolamna*	tooth	phospharenite	neritic	Campanian	75	148	151
P10	New Jersey, USA	*Scapanorhynchus*	tooth	sandstone	neritic	Upper Campanian	74	99.4	242
P11	Youssoufia, Morocco	*Cretolamna*	tooth	phospharenite	neritic	Maastrichtian	68	20.25	14.32
P12	Toro-toro, Bolivia	*Pucapristis*	tooth	phospharenite	neritic	Maastrichtian	68	282	503
P13a	Youssoufia, Morocco	*Myliobatis*	tooth	phospharenite	neritic	Dano-Montian	62	50.6	30.4
P14	Sididaoui, Morocco	*Striatolamia*	tooth	phospharenite	neritic	Early Ypresian	52	42.64	12.88
P15	North Peru	*Isurus*	tooth	sandstone	neritic	Middle Eocene	46	7.36	10.29
P16	Kpogame, Togo	*Synodontaspis*	tooth	phospharenite	neritic	Middle Eocene	46	8.48	9.21
P16a	Kpogame, Togo	*Synodontaspis*	tooth	phospharenite	neritic	Early Lutetian	46	82.2	108.3
P16c	Kpogame, Togo	Teleost vertebra	tooth	phospharenite	neritic	Early Lutetian	46	110	134
P16e	Kpogame, Togo	*Synodontaspis*	tooth	phospharenite	neritic	Middle Lutetian	45	34	46
P21	Al-Sarrar, Saudi Arabia	*Myliobatis*	tooth	sandstone	neritic	Burdigalian	16	1052	1390
P18b	Loupian, France	*Myliobatis*	tooth	phospharenite	neritic	Middle Miocene	14	28.4	30.1
P19	Bonpas, France	*Mitsukurina*	tooth	sandstone	bathyal	Middle Miocene	14	468	549
P20	Sacaco, Peru	*Carcharocles*	tooth	sandstone	neritic	Early Pliocene	5	0.624	1.244
P22	Pichegu, France	*Synodontaspis*	tooth	clay	neritic/ bathyal	Middle Pliocene	3	15.6	30.5
Grandjean (1989)									
Cou23-24Aa	Coumiac, France	unidentified	conodont	limestone	neritic	Frasnian	365	11.63	37.4

Pr (ppm)	Nd (ppm)	Sm (ppm)	Eu (ppm)	Gd (ppm)	Tb (ppm)	Dy (ppm)	Ho (ppm)	Er (ppm)	Tm (ppm)	Yb (ppm)	Lu (ppm)	Σ(La + Sm + Yb)	(La/Sm) N	(Sm/Yb) N	Analytical method
	290	163	34	181		102		30		17	2.3	245	0.07	5.21	Isotopic dilution, TIMS
	151.7	27.18		30.3		25.9		13.18		7.14	0.67	293.32	1.70	2.07	Isotopic dilution, TIMS
	343	57.4	12	56.9		42.87		24.9		25		626.4	1.69	1.25	Isotopic dilution, TIMS
	706	147	28	115		98		28		13.8	1.72	631.8	0.57	5.79	Isotopic dilution, TIMS
	367	80.3	18	78		58.7		17.6		9	1.07	332.3	0.54	4.85	Isotopic dilution, TIMS
	718	126	23.2	85		83		36		24.7	3.04	869.7	1.02	2.77	Isotopic dilution, TIMS
	74	12.93	2.93	14.5		15.3		10.8		9.2	1.42	170.13	2.04	0.76	Isotopic dilution, TIMS
	81.3	15.75	3.39	16.14		14.1		7.87		7.23	1.02	122.38	1.12	1.18	Isotopic dilution, TIMS
	13	2.45	0.661	3.32		3.77		3.21		3.39	0.52	26.09	1.47	0.39	Isotopic dilution, TIMS
	208.4	38.5	9.23	38.3		45.5		29.7		23	3.03	343.5	1.30	0.91	Isotopic dilution, TIMS
	32.2	6.31	1.86	9.22		9.62		7.72		7.87	0.98	64.78	1.43	0.44	Isotopic dilution, TIMS
	25.6	4.86	1.27	6.77		6.91		5.46		5.56	0.85	53.06	1.56	0.48	Isotopic dilution, TIMS
	3.76	0.731	0.31	1.43		1.45		1		1.16	0.18	9.251	1.79	0.34	Isotopic dilution, TIMS
	2.88	0.496	0.16	0.94		1.1		1.25		1.43	0.22	10.406	3.05	0.19	Isotopic dilution, TIMS
	39.6	39.6	2.11	9.96		9.94		6.43		6.95	1.07		0.37	3.10	Isotopic dilution, TIMS
	41	7.4	2.71	12.88		13.99		11.8		13.9	2.18	131.3	2.65	0.29	Isotopic dilution, TIMS
	19	3.5	0.98	4.71		5.24		4.54		4.63	0.8	42.13	1.73	0.41	Isotopic dilution, TIMS
	11.116	224.5	53.1	147.6		122.5		74		59	9	1335.5	0.83	2.07	Isotopic dilution, TIMS
	11	1.89	0.51	2.75		3.05		2.35		3.08	0.4	33.37	2.68	0.33	Isotopic dilution, TIMS
	252	43	11.5	52		52.6		30		25	3.3	536	1.94	0.94	Isotopic dilution, TIMS
	0.651	0.136	0.025	0.115		0.103		0.061		0.055	0.008	0.815	0.82	1.34	Isotopic dilution, TIMS
	16.5	5.14	1.55	5.59		6.75		3.96		3.21	0.48	23.95	0.54	0.87	Isotopic dilution, TIMS
	28.2	8.23	2.33	13.1		6.88		1.83		1.15		21.01	0.25	3.90	Ion probe, Cameca 3f

(continued on next page)

Table 2 (*continued*)

Samples	Location	Taxon	Material	Lithology	Environment	Period/stage	Proposed age (Ma)	La (ppm)	Ce (ppm)
Grandjean (1989)									
Cou23-24Ab	Coumiac, France	unidentified	conodont	limestone	neritic	Frasnian	365	19.6	66.8
Cou23-24Ac	Coumiac, France	unidentified	conodont	limestone	neritic	Frasnian	365	8.77	30
Cou23-24Ad	Coumiac, France	unidentified	conodont	limestone	neritic	Frasnian	365	12.2	43.4
Cou23-24Ae	Coumiac, France	unidentified	conodont	limestone	neritic	Frasnian	365	8.75	31.1
Cou23-24Af	Coumiac, France	unidentified	conodont	limestone	neritic	Frasnian	365	16.3	55
Cou24Ba	Coumiac, France	unidentified	conodont	limestone	neritic	Frasnian	365	3.61	18.7
Cou24Bb	Coumiac, France	unidentified	conodont	limestone	neritic	Frasnian	365	8.79	44.4
Cou24Bc	Coumiac, France	unidentified	conodont	limestone	neritic	Frasnian	365	8.56	39.3
Cou24Bd	Coumiac, France	unidentified	conodont	limestone	neritic	Frasnian	365	3.75	20.7
Cou24Be	Coumiac, France	unidentified	conodont	limestone	neritic	Frasnian	365	11.2	42.4
Cou24Bf	Coumiac, France	unidentified	conodont	limestone	neritic	Frasnian	365	5.23	23.1
Cou24Bg	Coumiac, France	unidentified	conodont	limestone	neritic	Frasnian	365	4.42	13
Cou24Bh	Coumiac, France	unidentified	conodont	limestone	neritic	Frasnian	365	6.45	19.5
Cou31Ga	Coumiac, France	unidentified	conodont	limestone	neritic	Famennian	360	15.7	35.4
Cou31Gb1	Coumiac, France	unidentified	conodont	limestone	neritic	Famennian	360	11.4	32.4
Cou31Gb2	Coumiac, France	unidentified	conodont	limestone	neritic	Famennian	360	11.8	32
Cou31Gb3	Coumiac, France	unidentified	conodont	limestone	neritic	Famennian	360	12.2	35.2
Cou31Gc1	Coumiac, France	unidentified	conodont	limestone	neritic	Famennian	360	8.53	24
Cou31Gc2	Coumiac, France	unidentified	conodont	limestone	neritic	Famennian	360	7.79	19.8
Cou31Gd	Coumiac, France	unidentified	conodont	limestone	neritic	Famennian	360	2.56	8.68
Cou31Ge	Coumiac, France	unidentified	conodont	limestone	neritic	Famennian	360	4.3	12.4
Cou31Gf	Coumiac, France	unidentified	conodont	limestone	neritic	Famennian	360	6.09	13.9
Cou32A-Ba1	Coumiac, France	unidentified	conodont	limestone	neritic	Famennian	360	8.74	28.2
Cou32A-Ba2	Coumiac, France	unidentified	conodont	limestone	neritic	Famennian	360	8.44	26.9
Cou32A-Ba3	Coumiac, France	unidentified	conodont	limestone	neritic	Famennian	360	7.67	23.8

Pr (ppm)	Nd (ppm)	Sm (ppm)	Eu (ppm)	Gd (ppm)	Tb (ppm)	Dy (ppm)	Ho (ppm)	Er (ppm)	Tm (ppm)	Yb (ppm)	Lu (ppm)	Σ(La + Sm + Yb)	(La/Sm) N	(Sm/Yb) N	Analytical method
	45	11.6	3.23	19		9.15		2.25		1.78		32.98	0.30	3.54	Ion probe, Cameca 3f
	23.4	6.48	1.96	10.8		4.59		1.26		0.78		16.03	0.24	4.53	Ion probe, Cameca 3f
	30.5	9.07	2.86	15.4		8.48		2.12		1.78		23.05	0.24	2.76	Ion probe, Cameca 3f
	26.6	7.1	2.37	11.9		6.28		1.48		1.23		17.08	0.22	3.14	Ion probe, Cameca 3f
	40.1	11.7	3.51	19.7		9.48		2.62		2.08		30.08	0.25	3.07	Ion probe, Cameca 3f
	22.4	8.3	2.3	12.5		4.85		1.43		0.97		12.88	0.08	4.71	Ion probe, Cameca 3f
	54.4	20.5	5.7	25.8		14.4		3.82		2.4		31.69	0.08	4.63	Ion probe, Cameca 3f
	43.7	15.7	4.6	19.2		10.6		3.04		2.15		26.41	0.10	3.94	Ion probe, Cameca 3f
	27.4	9.73	2.42	12		6.85		1.68		1.08		14.56	0.07	4.84	Ion probe, Cameca 3f
	42.3	21.2	6.35	29		14.3		4.03		3		35.4	0.09	3.83	Ion probe, Cameca 3f
	20.7	10.1	3.09	13.5		6.06		1.59		1.28		16.61	0.09	4.28	Ion probe, Cameca 3f
	27.2	10.5	2.91	15.6		9.24		2.64		1.94		16.86	0.07	2.95	Ion probe, Cameca 3f
	34.7	12.2	3.54	16.8		11.7		2.83		2.1		20.75	0.09	3.15	Ion probe, Cameca 3f
	65.6	28.7	8	33.2		16.4		5.69		4.03		48.43	0.10	3.86	Ion probe, Cameca 3f
	57.3	23	6.25	31.3		14		4.4		3.04		37.44	0.09	4.08	Ion probe, Cameca 3f
	58.2	18.7	6.4	31.2		12.8		3.61		2.63		33.13	0.11	3.88	Ion probe, Cameca 3f
	50.1	23.5	7	32		14.3		4.12		3.28		38.98	0.09	3.89	Ion probe, Cameca 3f
	35.8	14.8	4.78	20.9		10.7		3.24		2.53		25.86	0.10	3.16	Ion probe, Cameca 3f
	35.5	17.3	5.29	23.8		11.3		2.92		2.29		27.38	0.08	4.11	Ion probe, Cameca 3f
	12.3	6.48	1.6	8.25		3.95		1.33		0.82		9.86	0.07	4.24	Ion probe, Cameca 3f
	21.7	9.31	2.9	14.6		6.38		1.77		1.29		14.9	0.08	3.94	Ion probe, Cameca 3f
	19	8.93	2.19	13		7.41		2.35		1.56		16.58	0.12	3.12	Ion probe, Cameca 3f
	60.1	30.3	7.92	38.5		21.8		6.94		4.01		43.05	0.05	4.09	Ion probe, Cameca 3f
	55	27.9	7.18	37.2		19		6.56		4.11		40.45	0.05	3.72	Ion probe, Cameca 3f
	47.3	28	7.78	37.8		20.8		6.03		3.07		38.74	0.05	5.04	Ion probe, Cameca 3f

(continued on next page)

Table 2 (*continued*)

Samples	Location	Taxon	Material	Lithology	Environment	Period/stage	Proposed age (Ma)	La (ppm)	Ce (ppm)
Grandjean (1989)									
Cou32A-Bb	Coumiac, France	unidentified	conodont	limestone	neritic	Famennian	360	6.14	19
Cou32A-Bc	Coumiac, France	unidentified	conodont	limestone	neritic	Famennian	360	11.9	32.9
Cou32A-Bd	Coumiac, France	unidentified	conodont	limestone	neritic	Famennian	360	11.9	35.5
Cou32Ca	Coumiac, France	unidentified	conodont	limestone	neritic	Famennian	360	14.4	31.2
Cou32Cb	Coumiac, France	unidentified	conodont	limestone	neritic	Famennian	360	8.94	18.6
Cou32Cc	Coumiac, France	unidentified	conodont	limestone	neritic	Famennian	360	9.96	20.4
Cou32Cd	Coumiac, France	unidentified	conodont	limestone	neritic	Famennian	360	9.09	23.3
Cou32Ce	Coumiac, France	unidentified	conodont	limestone	neritic	Famennian	360	10.5	16.7
Cou34a	Coumiac, France	unidentified	conodont	limestone	neritic	Famennian	360	1.09	6.18
Cou34b	Coumiac, France	unidentified	conodont	limestone	neritic	Famennian	360	4.59	20.7
Cou34c	Coumiac, France	unidentified	conodont	limestone	neritic	Famennian	360	1.46	7.52
Bertram et al. (1992)									
Thelodont	Prior's Frome, UK	Thelodont	dermal denticles	limestone	platform	Ludfordian	411	1420	4920
Thelodont	Prior's Frome, UK	Thelodont	dermal denticles	limestone	platform	Ludfordian	411	2280	5380
Thelodont	Prior's Frome, UK	Thelodont	dermal denticles	limestone	platform	Ludfordian	411	1800	3550
Panderodus	Prior's Frome, UK	*Panderodus*	conodont	limestone	platform	Ludfordian	411	622	1590
Panderodus	Prior's Frome, UK	*Panderodus*	conodont	limestone	platform	Ludfordian	411	587	1460
Panderodus	Prior's Frome, UK	*Panderodus*	conodont	limestone	platform	Ludfordian	411	649	1650
Ozarkodina	Prior's Frome, UK	*Ozarkodina*	conodont	limestone	platform	Ludfordian	411	151	365
Ozarkodina	Prior's Frome, UK	*Ozarkodina*	conodont	limestone	platform	Ludfordian	411	53.8	128
Ozarkodina	Prior's Frome, UK	*Ozarkodina*	conodont	limestone	platform	Ludfordian	411	52.1	125
Ozarkodina	Prior's Frome, UK	*Ozarkodina*	conodont	limestone	platform	Ludfordian	411	120	291
Ozarkodina	Prior's Frome, UK	*Ozarkodina*	conodont	limestone	platform	Ludfordian	411	34.6	77.5
Dentacodina	Prior's Frome, UK	*Dentacodina*	conodont	limestone	platform	Ludfordian	411	716	1810
Dentacodina	Prior's Frome, UK	*Dentacodina*	conodont	limestone	platform	Ludfordian	411	642	1590

Pr (ppm)	Nd (ppm)	Sm (ppm)	Eu (ppm)	Gd (ppm)	Tb (ppm)	Dy (ppm)	Ho (ppm)	Er (ppm)	Tm (ppm)	Yb (ppm)	Lu (ppm)	Σ(La + Sm + Yb)	(La/Sm) N	(Sm/Yb) N	Analytical method
	36	21.4	6.19	28.6		15		4.56		2.06		29.6	0.05	5.59	Ion probe, Cameca 3f
	65.7	38.7	10.6	46.9		28		9.39		5.59		56.19	0.06	3.74	Ion probe, Cameca 3f
	69.4	40.9	11.5	53.4		29.7		8.82		4.79		57.59	0.05	4.65	Ion probe, Cameca 3f
	45.3	16.6	4.98	21.1		12.2		3.42		2.04		33.04	0.15	4.41	Ion probe, Cameca 3f
	26.9	10.1	2.92	14.7		7.41		2.19		1.47		20.51	0.16	3.72	Ion probe, Cameca 3f
	28.5	11	3.04	14.8		6.37		2.78		1.67		22.63	0.16	3.56	Ion probe, Cameca 3f
	28.1	9.89	2.83	13.4		6.61		2.33		1.22		20.2	0.16	4.40	Ion probe, Cameca 3f
	26.4	9.9	2.69	11.8		7.23		2.27		1.47		21.87	0.19	3.66	Ion probe, Cameca 3f
	11	7.27	3.14	16.2		6.28		1.72		1.18		9.54	0.03	3.34	Ion probe, Cameca 3f
	27.5	19.6	5.94	29.1		15.2		5.14		3.66		27.85	0.04	2.96	Ion probe, Cameca 3f
	11.7	7.13	3.51	19.3		7.02		2.01		1.49		10.08	0.04	2.66	Ion probe, Cameca 3f
	2780	551	224	514		380		175		79.2	5.87	2050.2	0.46	3.78	Isotope dilution, TIMS
	2690	555	160	624		461		193		86.4	9.62	2921.4	0.73	3.49	Isotope dilution, TIMS
	2850	554	196	534		432		190		86.4	9.55	2440.4	0.58	3.49	Isotope dilution, TIMS
	802	180	47.2	187		148		63.9		33.3	2.7	835.3	0.62	2.94	Isotope dilution, TIMS
	758	172	44.3	183		143		61.8		31.6	3.72	790.6	0.61	2.96	Isotope dilution, TIMS
	863	193	49.5	203		162		68.1		35.3	4.47	877.3	0.60	2.97	Isotope dilution, TIMS
	193	43	11.6	44.3		33.7		14.4		7.27	0.84	201.27	0.63	3.22	Isotope dilution, TIMS
	66.5	15.4	4.19	16.5		14.4		5.93		3.08	0.48	72.28	0.62	2.72	Isotope dilution, TIMS
	67.2	15.4	4.22	16.3		12.5		5.52		2.99	0.31	70.49	0.60	2.80	Isotope dilution, TIMS
	142	30.4	8.38	33.1		26.4		11.9		6.27	0.7	156.67	0.70	2.64	Isotope dilution, TIMS
	39.9	9.34	2.52	10.5		7.41		3.33		1.82	0.22	45.76	0.66	2.79	Isotope dilution, TIMS
	968	208	63.4	210		164		68.1		33.4	3.72	957.4	0.61	3.39	Isotope dilution, TIMS
	820	179	48	201		157		65.1		33.3	4.17	854.3	0.64	2.92	Isotope dilution, TIMS

(continued on next page)

Table 2 (*continued*)

Samples	Location	Taxon	Material	Lithology	Environment	Period/stage	Proposed age (Ma)	La (ppm)	Ce (ppm)
Grandjean et al. (1988)									
NFS4	Khouribga, Morocco	*Myliobatis*	tooth	phospharenite	neritic	Thanetian	57	34.5	15.4
NFS5	Sididaoui, Morocco	*Striatolamia*	tooth	phospharenite	neritic	Ypresian	53	47.2	15.3
NFS6	Sididaoui, Morocco	*Myliobatis*	tooth	phospharenite	neritic	Ypresian	53	46.7	14.7
SFS2	Adrar Mgorn, Morocco	*Physogaleus*	tooth	clay	neritic	Ypresian	53	84	131
SFS7	Adrar Mgorn, Morocco	Teleost	vertebra	clay	neritic	Thanetian	57	75.1	115
SFS121	Garitas, Western Sahara	Teleost	vertebra	sandstone	littoral	Upper Eocene	40	22.3	29.7
SFS122	Garitas, Western Sahara	Teleost	vertebra	sandstone	littoral	Upper Eocene	40	12.4	12.4
SFS123	Garitas, Western Sahara	Teleost	vertebra	sandstone	littoral	Upper Eocene	40	12.1	9.37
SFS1	Matam Seme, Senegal	*Myliobatis*	tooth	phospharenite	neritic	Ypresian	53	52	77
SFS3	Matam Seme, Senegal	*Eotoperdo*	tooth	phospharenite	neritic	Upper Thanetian	55	683	1971
SFS9	Matam Seme, Senegal	*Myliobatis*	tooth	phospharenite	neritic	Ypresian	53	73.5	112
SFS8	Sessao, Niger	*Myliobatis*	tooth	phospharenite	neritic	Thanetian	57	125	185
SFS10	Mont Igdaman, Niger	Teleost	vertebra	phospharenite	neritic	Maastrichtian	67	110	190
SFS10a	Mont Igdaman, Niger	Teleost	vertebra	phospharenite	neritic	Maastrichtian	67	58.9	100
PI11	Oron Givat Mador, Israel	*Cretolamna*	tooth	phospharenite	neritic	Maastrichtian	67	36.9	11.5
Elderfield and Pagett (1986)									
PD15-18	Peru/Chile	ichthyolith	tooth	not precised	shelf	Quaternary	1	1.13	1.36
PD18-30	Peru/Chile	ichthyolith	tooth	not precised	shelf	Quaternary	1	3.48	6.19
SG46-47	Tyrrhenian Sea	ichthyolith	tooth	not precised	shelf	Quaternary	1	16.8	130
CIR170	Namibia	ichthyolith	tooth	not precised	shelf	Quaternary	1	48.9	110
CIR170 verteb.	Namibia	ichthyolith	vertebra	not precised	shelf	Quaternary	1	63.6	458
CIR175	Namibia	ichthyolith	tooth	not precised	shelf	Quaternary	1	36	113
CIR175 verteb.	Namibia	ichthyolith	vertebra	not precised	shelf	Quaternary	1	107	413
CK(80)1	Cook Islands	ichthyolith	tooth	not precised	open sea	Quaternary	1	74.7	6.9

Pr (ppm)	Nd (ppm)	Sm (ppm)	Eu (ppm)	Gd (ppm)	Tb (ppm)	Dy (ppm)	Ho (ppm)	Er (ppm)	Tm (ppm)	Yb (ppm)	Lu (ppm)	Σ(La + Sm + Yb)	(La/Sm) N	(Sm/Yb) N	Analytical method
	17.7	3.32	0.9	4.81		5.24		4.54		4.67		42.49	1.85	0.39	Isotope dilution, TIMS
	27	5.08	1.38	7.53		7.86		6.43		6.28	1.03	58.56	1.66	0.44	Isotope dilution, TIMS
	28.1	5.34	1.49	7.88		8.16		6.51		6.22		58.26	1.56	0.47	Isotope dilution, TIMS
	62.1	11.7	2.83	12.4		10.5		5.56		3.75		99.45	1.28	1.70	Isotope dilution, TIMS
	54	10.2	2.29	10.7		9.29		5.81		4.19		89.49	1.31	1.32	Isotope dilution, TIMS
	13.2	2.49	0.64	2.68		2.62		1.91		2.21		27	1.60	0.61	Isotope dilution, TIMS
	4.27	0.73	0.23	0.89		1.11		0.94		0.86		13.99	3.03	0.46	Isotope dilution, TIMS
	4.55	0.85	0.24	0.99		1.08		0.87		0.94		13.89	2.54	0.49	Isotope dilution, TIMS
	30.4	5.14	1.29	5.61		5.6		4.16		4.29		61.43	1.80	0.65	Isotope dilution, TIMS
	935	225	60.1	259		241		134		105		1013	0.54	1.17	Isotope dilution, TIMS
	49.8	8.96	2.27	9.52		9.48		6.67		6.38	1.02	88.84	1.46	0.76	Isotope dilution, TIMS
	81	17.1	4.73	24.4		28.8		22.3		22		164.1	1.30	0.42	Isotope dilution, TIMS
	97.3	20.9	5.92	28.7		30.3		20.4		16.5	2.5	147.4	0.94	0.69	Isotope dilution, TIMS
	57	13	3.67	19.2		17.8		12.3		15.8		87.7	0.81	0.45	Isotope dilution, TIMS
	14.7	2.86	0.85	5.17		6.7		6.96		7.54		47.3	2.30	0.21	Isotope dilution, TIMS
	0.78	0.13	0.03			0.19		0.19		0.2		1.46	1.55	0.35	Isotope dilution, TIMS
	2.91	0.58	0.14	0.66		0.61		0.54		0.52		4.58	1.07	0.61	Isotope dilution, TIMS
	30	5	12	6				7		7		28.8	0.60	0.39	Isotope dilution, TIMS
	40.6	8.5	2.03	10.7		10		6		8		65.4	1.02	0.58	Isotope dilution, TIMS
	88.9	19.5	4.6			28		14		15		98.1	0.58	0.71	Isotope dilution, TIMS
	48.3	10.3	2.57	13.3				7.9		7.2		53.5	0.62	0.78	Isotope dilution, TIMS
	129	30	6.8	34.6		35.7		18.9		16.8		153.8	0.64	0.97	Isotope dilution, TIMS
	81.6	18.1	4.55	22		21.3		13.7		11.9		104.7	0.74	0.83	Isotope dilution, TIMS

(continued on next page)

Table 2 (*continued*)

Samples	Location	Taxon	Material	Lithology	Environment	Period/stage	Proposed age (Ma)	La (ppm)	Ce (ppm)
Elderfield and Pagett (1986)									
DWHD16	Pacific Ocean, 16°S–145°W	ichthyolith	tooth	not precised	open sea	Quaternary	1	170	9.5
PLDG FFG 0.01	Pacific Ocean, 11°N–140°W	ichthyolith	tooth	not precised	open sea	Quaternary	1	187	66.1
9940k40-45	Cape Basin, 34°S–9°E	ichthyolith	tooth	not precised	open sea	Quaternary	1	291	216
9940k90-100	Cape Basin, 34°S–9°E	ichthyolith	tooth	not precised	open sea	Quaternary	1	259	181
9940k150-160	Cape Basin, 34°S–9°E	ichthyolith	tooth	not precised	open sea	Quaternary	1	866	750
9942	Cape Basin, 34°S–7°E	ichthyolith	tooth	not precised	open sea	Quaternary	1	238	30.6
Kemp and Trueman (2003)									
SC-24	Solnhofen, Germany	*Lumbricaria recta*	coprolith	limestone	lagoon	Tithonian	145	23.77	41.58
SC-32	Solnhofen, Germany	*Lumbricaria recta*	coprolith	limestone	lagoon	Tithonian	145	57.32	106.1
SC-38	Solnhofen, Germany	*Lumbricaria recta*	coprolith	limestone	lagoon	Tithonian	145	55.64	96.12
SC-76	Solnhofen, Germany	*Lumbricaria recta*	coprolith	limestone	lagoon	Tithonian	145	39.79	85.09
SC-122	Solnhofen, Germany	*Lumbricaria recta*	coprolith	limestone	lagoon	Tithonian	145	28.94	63.29
I 29	Solnhofen, Germany	*Lumbricaria recta*	coprolith	limestone	lagoon	Tithonian	145	93.26	153.1
II 6	Solnhofen, Germany	*Lumbricaria recta*	coprolith	limestone	lagoon	Tithonian	145	37.66	65.84
III 38	Solnhofen, Germany	*Lumbricaria recta*	coprolith	limestone	lagoon	Tithonian	145	95.75	180.1
III 69	Solnhofen, Germany	*Lumbricaria recta*	coprolith	limestone	lagoon	Tithonian	145	74.72	127.7
III 96	Solnhofen, Germany	*Lumbricaria recta*	coprolith	limestone	lagoon	Tithonian	145	35.33	61.32
III 128	Solnhofen, Germany	*Lumbricaria recta*	coprolith	limestone	lagoon	Tithonian	145	20.65	37.07
III 129	Solnhofen, Germany	*Lumbricaria recta*	coprolith	limestone	lagoon	Tithonian	145	4.71	7.74
III 244	Solnhofen, Germany	*Lumbricaria recta*	coprolith	limestone	lagoon	Tithonian	145	62.52	109.5
IV 69	Solnhofen, Germany	*Lumbricaria recta*	coprolith	limestone	lagoon	Tithonian	145	25.27	43.6
IV 196	Solnhofen, Germany	*Lumbricaria recta*	coprolith	limestone	lagoon	Tithonian	145	58.22	107.2
IV 200	Solnhofen, Germany	*Lumbricaria recta*	coprolith	limestone	lagoon	Tithonian	145	66.8	115
IV 688	Solnhofen, Germany	*Lumbricaria recta*	coprolith	limestone	lagoon	Tithonian	145	24.45	40.19
IV 847	Solnhofen, Germany	*Lumbricaria recta*	coprolith	limestone	lagoon	Tithonian	145	65.58	110.3

Pr (ppm)	Nd (ppm)	Sm (ppm)	Eu (ppm)	Gd (ppm)	Tb (ppm)	Dy (ppm)	Ho (ppm)	Er (ppm)	Tm (ppm)	Yb (ppm)	Lu (ppm)	Σ(La + Sm + Yb)	(La/Sm) N	(Sm/Yb) N	Analytical method
	105	19.2	5.24	28.4		27.6		21.6		17.5		206.7	1.58	0.60	Isotope dilution, TIMS
	292	68.8	18.2	64.6		53.6		24.8		18.9		274.7	0.48	1.98	Isotope dilution, TIMS
	532	136	43.1	136		164		76		69		496	0.38	1.07	Isotope dilution, TIMS
	426	113	26	110		113		69		57		429	0.41	1.08	Isotope dilution, TIMS
	1460	372	87	376		375		203		196		1434	0.41	1.03	Isotope dilution, TIMS
	267	57.8	13.6	62.9		56.4		32.4		26.7		322.5	0.73	1.18	Isotope dilution, TIMS
7.69	33.2	10.56	2.23	11.86	1.85	9.24	1.87	4.4	0.57	2.11	0.39	36.44	0.40	2.72	ICP-MS
18.67	72.4	18.9	4.72	24.95	3.7	20.06	4.11	9.55	1.13	4.17	0.68	80.39	0.54	2.46	ICP-MS
17.79	71	20.36	4.63	25.49	3.94	22.31	4.18	10.41	1.28	4.76	0.77	80.76	0.49	2.33	ICP-MS
14.03	56.9	16.46	3.71	18.88	2.97	15.57	2.96	7.27	0.96	3.4	0.54	59.65	0.43	2.63	ICP-MS
10.9	44.1	11.91	3.04	13.83	2.15	11.65	2.28	5.51	0.69	2.65	0.4	43.5	0.43	2.44	ICP-MS
29.86	127	32.16	7.2	42.38	5.18	28.87	5.55	12.28	1.4	4.73	0.72	130.15	0.52	3.70	ICP-MS
11.15	51.5	13.12	2.83	17.44	2.21	12.81	2.17	4.88	0.54	2.26	0.25	53.04	0.51	3.16	ICP-MS
32.85	143	35.79	8.47	49.53	6.35	35	6.57	15.52	1.53	6.31	0.79	137.85	0.48	3.08	ICP-MS
22.75	93.4	24.17	5.29	31.57	3.99	22.56	4.22	9.73	1.07	4.58	0.53	103.47	0.55	2.87	ICP-MS
11.5	49.4	12.43	2.67	16.46	2.13	12.37	2.3	5.56	0.52	2.21	0.31	49.97	0.51	3.06	ICP-MS
7.07	35.1	8.93	2.22	12.32	1.69	9.27	1.74	3.89	0.42	1.52	0.2	31.1	0.41	3.20	ICP-MS
1.55	6.06	1.99	0.38	2.16	0.24	1.6	0.31	0.74	0.1	0.29	0.05	6.99	0.42	3.73	ICP-MS
19.29	85.5	20.59	4.99	29.86	3.86	22.92	4.53	10.39	1.14	4.54	0.56	87.65	0.54	2.47	ICP-MS
7.86	34.8	8.69	1.95	12.62	1.64	9.34	1.82	4.32	0.45	1.75	0.23	35.71	0.52	2.70	ICP-MS
20.43	89.9	21.43	4.87	28.77	3.55	19.39	3.46	8.61	0.87	3.25	0.43	82.9	0.48	3.59	ICP-MS
21.74	91.4	22.93	5.27	30.5	4.29	23.55	4.55	10.57	1.14	4.35	0.61	94.08	0.52	2.87	ICP-MS
7.59	34.3	9.38	2.15	12.09	1.68	9.38	1.9	4.1	0.42	1.67	0.2	35.5	0.46	3.05	ICP-MS
20.76	86.1	21.94	4.84	28.6	3.67	20.45	3.63	8.86	0.9	3.7	0.42	91.22	0.53	3.22	ICP-MS

(continued on next page)

Table 2 (*continued*)

Samples	Location	Taxon	Material	Lithology	Environment	Period/stage	Proposed age (Ma)	La (ppm)	Ce (ppm)
Kemp and Trueman (2003)									
IV 880	Solnhofen, Germany	*Lumbricaria recta*	coprolith	limestone	lagoon	Tithonian	145	7.77	12.44
IV 1030	Solnhofen, Germany	*Lumbricaria recta*	coprolith	limestone	lagoon	Tithonian	145	108.2	173.9
V 53	Solnhofen, Germany	*Lumbricaria recta*	coprolith	limestone	lagoon	Tithonian	145	25.08	38.99
V 128	Solnhofen, Germany	*Lumbricaria recta*	coprolith	limestone	lagoon	Tithonian	145	40.79	71.39
V 188	Solnhofen, Germany	*Lumbricaria recta*	coprolith	limestone	lagoon	Tithonian	145	40.64	65.24
V 222	Solnhofen, Germany	*Lumbricaria recta*	coprolith	limestone	lagoon	Tithonian	145	52.56	88.97
V 397	Solnhofen, Germany	*Lumbricaria recta*	coprolith	limestone	lagoon	Tithonian	145	74	138.1
V 444	Solnhofen, Germany	*Lumbricaria recta*	coprolith	limestone	lagoon	Tithonian	145	67.11	117.8
V 510	Solnhofen, Germany	*Lumbricaria recta*	coprolith	limestone	lagoon	Tithonian	145	55.35	95.66
V 585	Solnhofen, Germany	*Lumbricaria recta*	coprolith	limestone	lagoon	Tithonian	145	52.59	90.58
V 608	Solnhofen, Germany	*Lumbricaria recta*	coprolith	limestone	lagoon	Tithonian	145	44.57	79.57
V 611	Solnhofen, Germany	*Lumbricaria recta*	coprolith	limestone	lagoon	Tithonian	145	50.49	87.64
VI 80_1	Solnhofen, Germany	*Lumbricaria recta*	coprolith	limestone	lagoon	Tithonian	145	84.4	121.4
VI 105	Solnhofen, Germany	*Lumbricaria recta*	coprolith	limestone	lagoon	Tithonian	145	34.38	57.32
FL_1	Solnhofen, Germany	fish	bone	limestone	lagoon	Tithonian	145	13.22	18.38
FL_2	Solnhofen, Germany	*Lumbricaria recta*	coprolith	limestone	lagoon	Tithonian	145	20.27	33.75
FL_3	Solnhofen, Germany	fish	soft tissue	limestone	lagoon	Tithonian	145	33.63	61.71
PL_1	Solnhofen, Germany	fish	bone	limestone	lagoon	Tithonian	145	74.55	147.1
PT_1	Solnhofen, Germany	fish	bone	limestone	lagoon	Tithonian	145	35.73	61.16
PT_2	Solnhofen, Germany	fish	bone	limestone	lagoon	Tithonian	145	27.57	46.85
Z_1	Solnhofen, Germany	fish	bone	limestone	lagoon	Tithonian	145	12.17	10.58
Z_2	Solnhofen, Germany	*Lumbricaria recta*	coprolith	limestone	lagoon	Tithonian	145	92.35	104.1
BL_5	Solnhofen, Germany	*Lumbricaria recta*	coprolith	limestone	lagoon	Tithonian	145	55.17	102.4
BL_6	Solnhofen, Germany	*Lumbricaria recta*	coprolith	limestone	lagoon	Tithonian	145	36.24	62.26

Pr (ppm)	Nd (ppm)	Sm (ppm)	Eu (ppm)	Gd (ppm)	Tb (ppm)	Dy (ppm)	Ho (ppm)	Er (ppm)	Tm (ppm)	Yb (ppm)	Lu (ppm)	Σ(La+Sm+Yb)	(La/Sm) N	(Sm/Yb) N	Analytical method
2.42	10.6	2.6	0.75	3.68	0.55	2.31	0.53	1.5	0.16	0.4	0.13	10.77	0.53	3.54	ICP-MS
36.17	144	34.38	9.1	46.62	6.12	36.47	6.06	15.81	1.61	6.45	0.88	149.03	0.56	2.90	ICP-MS
7	28.2	7.45	1.49	10.37	1.31	7.96	1.53	3.59	0.38	1.47	0.2	34	0.60	2.76	ICP-MS
13.09	57.8	14.65	3.67	22.24	3	16.6	3.36	7.32	0.79	2.81	0.36	58.25	0.50	2.84	ICP-MS
12.84	58.8	14.29	3.63	20.81	2.93	15.74	3.14	7.32	0.75	3.01	0.42	57.94	0.51	2.58	ICP-MS
17.4	78.5	19.8	4.88	28.63	3.77	21.18	4.1	10.05	1.01	3.72	0.52	76.08	0.47	2.89	ICP-MS
25.25	113	28.01	6.5	38.06	4.81	25.81	4.81	11.08	1.11	4.42	0.55	106.43	0.47	3.45	ICP-MS
22.42	97.1	23.88	5.74	34.02	4.63	25.64	4.89	11.29	1.22	4.45	0.58	95.44	0.50	2.92	ICP-MS
19.33	80.4	19.12	4.21	24.3	3.09	17.8	3.35	8.46	0.73	3.12	0.31	77.59	0.52	3.33	ICP-MS
18.23	80.2	20.06	4.78	26.69	3.67	20.98	3.93	9.55	0.91	3.35	0.45	76	0.47	3.26	ICP-MS
16.31	71.9	18.95	4.67	26.53	3.59	19.61	3.7	8.8	0.88	3.47	0.41	66.99	0.42	2.97	ICP-MS
15.42	64.9	16.07	4.06	24.48	3.24	18.26	3.56	7.96	0.86	3.37	0.4	69.93	0.56	2.59	ICP-MS
25.66	105	25.74	5.9	35.36	4.79	25.9	5.26	12.38	1.27	5.04	0.78	115.18	0.58	2.78	ICP-MS
11.09	50.9	13.29	2.96	17.86	2.18	12.67	2.2	5.1	0.54	2.03	0.27	49.7	0.46	3.56	ICP-MS
2.42	8.89	2.04	0.6	4.5	0.47	3.1	0.6	1.45	0.15	0.66	0.1	15.92	1.15	1.68	ICP-MS
5.4	22.3	6.39	1.57	8.13	1.3	6.52	1.33	3.47	0.55	1.64	0.29	28.3	0.57	2.12	ICP-MS
8.05	37.5	9.61	1.93	13.55	1.74	10.31	1.86	4.38	0.34	1.9	0.16	45.14	0.62	2.75	ICP-MS
16.55	73.7	16.5	3.63	24.92	3.19	19.15	3.39	8.15	0.71	3.46	0.3	94.51	0.80	2.59	ICP-MS
8.71	29	8.28	2.2	11.25	1.69	9.93	1.96	4.26	0.61	2.4	0.4	46.41	0.77	1.88	ICP-MS
7.28	27.6	7.61	1.94	10.27	1.58	9.56	1.78	4.33	0.55	2.26	0.41	37.44	0.65	1.83	ICP-MS
2.03	7.76	1.95	0.55	3.36	0.42	2.89	0.63	1.67	0.21	0.69	0.12	14.81	1.11	1.54	ICP-MS
24.1	92.4	21.49	5.54	29.58	4.03	22.68	4.83	12.54	1.6	5.85	0.98	119.69	0.77	2.00	ICP-MS
16.19	70.7	17.86	3.47	23.08	2.88	17.02	2.93	7.28	0.55	3.14	0.19	76.17	0.55	3.09	ICP-MS
9.72	42.7	10.95	2.18	16.38	2.01	12.3	2.21	5.36	0.38	2.2	0.08	49.39	0.59	2.71	ICP-MS

(continued on next page)

Table 2 (*continued*)

Samples	Location	Taxon	Material	Lithology	Environment	Period/stage	Proposed age (Ma)	La (ppm)	Ce (ppm)
Picard et al. (2002)									
93357	Stonesfield, UK	*Asteracanthus*	tooth	siliciclastic	protected	Early–Middle Bathonian	168	57.61	54.29
93362	St. Gaultier, France	*Asteracanthus*	tooth	carbonate	protected	Lower Bathonian	169	110.81	60.60
92154	Tonnerre, France	*Crocodilian*	tooth	carbonate	upper offshore	Lower Oxfordian	159	65.26	101.50
92210	St. Gaultier, France	*Machimosaurus*	tooth	carbonate	protected	Lower Bathonian	169	168.84	71.93
93369	Stonesfield, UK	*Crocodilian*	tooth	siliciclastic	protected	Early–Middle Bathonian	168	338.84	503.67
D8	Etrochey, France	*Crocodilian*	tooth	carbonate	upper offshore	Early Callovian	164	341.09	528.17
D19	Les Perrières, France	*Pycnodont*	tooth	carbonate	lower offshore	Lower Bathonian	169	744.25	597.28
D25	Dijon, France	*Asteracanthus*	tooth	carbonate	upper offshore	Early Callovian	164	363.68	753.01
93405	Calvados, France	Reptile	tooth	clay	upper offshore	Lower Callovian	164	413.05	1040.60
L13	Pagny, France	*Pycnodont*	tooth	clay	protected	Lower Oxfordian	159	2.16	4.47
Na6	Nantua, France	*Asteracanthus*	tooth	carbonate	upper offshore	Middle–Lower Bathonian	168	226.70	200.47
L10	Hurigny, France	*Asteracanthus*	tooth	carbonate	upper offshore	Lower Bajocian	176	311.66	334.34
L11	Hurigny, France	Reptile	tooth	carbonate	upper offshore	Lower Bajocian	176	606.34	773.08
D6	Vanvey, France	*Asteracanthus*	tooth	carbonate	shoreface	Middle Bathonian	167	6.20	9.39
D10	Etrochey, France	*Asteracanthus*	tooth	carbonate	upper offshore	Early Callovian	164	176.70	398.66
93364	Tonnerre, France	*Asteracanthus*	tooth	carbonate	upper offshore	Lower Oxfordian	159	13.07	22.01
Lécuyer et al. (2002)									
LE3	Laño, Spain	*Crocodilian*	tooth	clayey sand	littoral	Maastrichtian	68	15.53	12.93
LE8	Laño, Spain	Fish	scale	clayey sand	littoral	Maastrichtian	68	20.25	16.14
LT1	Laño, Spain	Shark	tooth	limestone	littoral	Maastrichtian	68	13.78	12.93
LL1	Laño, Spain	Turtle	plate	clayey sand	littoral	Maastrichtian	68	18.95	14.75
LL2	Laño, Spain	Dinosaur	bone	clayey sand	littoral	Maastrichtian	68	5.05	3.58
LL3	Laño, Spain	*Crocodilian*	vertebra	clayey sand	littoral	Maastrichtian	68	5.16	3.56
CB1	Cuesva, Spain	*Crocodilian*	osteoderm	argilites	littoral	Maastrichtian	68	11.47	30.72
CB2	Cuesva, Spain	Turtle	plate	argilites	littoral	Maastrichtian	68	7.04	24.22
US1	Urria, Spain	vertebrate	bone	argilites	littoral	Maastrichtian	68	2.41	6.54
US2	Urria, Spain	vertebrate	bone	argilites	littoral	Maastrichtian	68	3.12	6.91
US3	Urria, Spain	Turtle	plate	argilites	littoral	Maastrichtian	68	11.74	14.88
Lécuyer et al. (1998)									
OBN1	Estonia	*Ungula/ Schmidtites*	shell	phosphorite, sandstone	littoral	Lower Ordovician	490	173	413

Pr (ppm)	Nd (ppm)	Sm (ppm)	Eu (ppm)	Gd (ppm)	Tb (ppm)	Dy (ppm)	Ho (ppm)	Er (ppm)	Tm (ppm)	Yb (ppm)	Lu (ppm)	Σ(La + Sm + Yb)	(La/Sm) N	(Sm/Yb) N	Analytical method
5.16	18.84	2.47	0.61	3.89	0.50	3.12	0.77	2.21		1.62	0.24	61.7	3.39	0.78	ICP-MS
15.94	72.51	15.32	3.57	28.38	3.70	23.41	5.41	12.76		4.65	0.63	130.78	1.05	1.68	ICP-MS
17.20	72.50	14.17	2.77	18.66	2.72	15.63	3.17	7.47		3.09	0.41	82.52	0.67	2.33	ICP-MS
24.38	109.43	21.03	5.07	39.36	5.78	39.09	9.46	23.25		9.20	1.32	199.07	1.17	1.16	ICP-MS
50.29	176.94	22.70	5.52	27.31	4.14	26.67	6.11	16.98		11.08	1.51	372.62	2.17	1.04	ICP-MS
92.13	372.42	68.77	14.09	85.57	13.12	74.87	14.16	31.76		13.25	1.65	423.11	0.72	2.64	ICP-MS
155.79	611.98	106.63	20.98	124.14	16.72	90.52	16.83	35.57		11.88	1.39	862.76	1.01	4.56	ICP-MS
127.16	499.51	96.50	17.60	101.20	14.56	74.35	12.86	26.24		9.79	1.12	469.97	0.55	5.01	ICP-MS
130.19	491.92	83.42	17.27	79.93	12.17	68.16	12.97	30.48		16.42	2.15	512.89	0.72	2.58	ICP-MS
0.58	2.32	0.46	0.10	0.46	0.06	0.39	0.08	0.22		0.17	0.03	2.79	0.68	1.35	ICP-MS
38.89	141.16	22.58	4.44	26.96	3.93	21.20	3.91	8.19		2.55	0.27	251.83	1.46	4.49	ICP-MS
63.37	237.28	42.52	8.25	50.35	7.38	42.03	8.08	18.31		7.82	0.95	362	1.06	2.76	ICP-MS
153.10	615.22	120.18	23.69	133.63	19.68	113.34	22.30	54.05		28.15	3.47	754.67	0.73	2.17	ICP-MS
1.30	5.25	0.99	0.20	1.39	0.22	1.48	0.36	0.96		0.50	0.07	7.69	0.91	1.01	ICP-MS
62.68	246.56	46.82	8.71	51.44	7.59	40.30	7.22	15.17		5.75	0.69	229.27	0.55	4.14	ICP-MS
3.22	12.87	2.53	0.46	3.43	0.54	3.27	0.67	1.59		0.65	0.08	16.25	0.75	1.98	ICP-MS
13.86	14.22	18.56	24.11	24.11	21.35	19.79	17.88	16.02		11.70	10.98	45.78	0.84	1.59	ICP-MS
20.71	21.97	30.51	39.35	37.57	32.34	28.94	25.90	22.95		17.19	16.34	67.95	0.66	1.78	ICP-MS
13.32	14.76	18.96	24.43	27.85	23.94	22.48	20.19	16.46		8.91	8.35	41.66	0.73	2.13	ICP-MS
14.22	14.29	17.77	24.80	28.11	26.57	27.26	26.62	24.39		16.66	15.02	53.39	1.07	1.07	ICP-MS
3.68	3.63	4.49	6.24	5.89	5.34	5.37	5.47	5.41		4.54	4.59	14.08	1.13	0.99	ICP-MS
3.15	2.88	3.24	4.62	5.21	5.56	6.48	6.81	6.78		5.07	4.86	13.47	1.59	0.64	ICP-MS
47.08	65.76	121.37	141.92	162.79	132.94	104.43	77.51	54.03		23.27	19.64	156.11	0.09	5.22	ICP-MS
47.13	68.52	115.58	131.86	144.26	120.21	96.73	72.29	50.87		21.33	17.81	143.95	0.06	5.42	ICP-MS
14.25	30.91	87.85	116.76	139.53	102.03	77.22	58.99	41.76		18.38	15.71	108.64	0.03	4.78	ICP-MS
13.82	18.81	27.36	32.10	39.58	35.34	32.68	27.50	20.57		8.78	6.83	39.26	0.11	3.12	ICP-MS
33.92	38.36	48.95	59.18	70.82	57.86	47.36	35.81	24.52		10.32	8.58	71.01	0.24	4.75	ICP-MS
52.70	215	44.38	9.50	57.56	8.08	44.51	8.86	21.20		10.73	1.45	228.11	0.57	2.10	ICP-MS

(continued on next page)

Table 2 (*continued*)

Samples	Location	Taxon	Material	Lithology	Environment	Period/stage	Proposed age (Ma)	La (ppm)	Ce (ppm)
Lécuyer et al. (1998)									
OBB1	Estonia	*Ungula/ Schmidtites*	shell	phosphorite, sandstone	littoral	Lower Ordovician	490	168	378
OBB2	Estonia	*Ungula/ Schmidtites*	shell	phosphorite, sandstone	littoral	Lower Ordovician	490	188	429
ES1	Estonia	*Ungula/ Schmidtites*	shell	phosphorite, sandstone	littoral	Lower Ordovician	490	183	493
ES2	Estonia	*Ungula/ Schmidtites*	shell	phosphorite, sandstone	littoral	Lower Ordovician	490	222	543
ES3	Estonia	*Ungula/ Schmidtites*	shell	phosphorite, sandstone	littoral	Lower Ordovician	490	299	708
ES4	Russia	*Obolus apollinis*	shell	phosphorite, sandstone	littoral	Lower Ordovician	490	194	424
ES5	Estonia	*Ungula/ Schmidtites*	shell	phosphorite, sandstone	littoral	Lower Ordovician	490	88	169
ES6	Estonia	*Mickwitzia* sp.	shell	phosphorite, sandstone	littoral	Lower Cambrian	490	461	1624
ES7	Russia	*Obolus rebrovi*	shell	phosphorite, sandstone	littoral	Middle Cambrian	490	334	1188
ES8	Estonia	*Ungula/ Schmidtites*	shell	phosphorite, sandstone	littoral	Lower Ordovician	490	67	136
Cal1	New Caledonia	*Lingula anatina*	shell	sandstone	littoral	Holocene	0	0.133	0.261
Ha1	Hawaii	*Lingula reevei*	shell	sandstone	littoral	Holocene	0	0.097	0.231
Cr1	Costa Rica	*Glottidia audebarti*	shell	sandstone	littoral	Holocene	0	0.269	0.508
Jap1	Japan	*Lingula anatina*	shell	sandstone	littoral	Holocene	0	0.280	0.389
LC	New Caledonia	*Lingula anatina*	shell	sandstone	estuary	Holocene	0	1.630	3.492
This study									
PC21	Puchevillers, France	undetermined fish	tooth	limestone	platform		82.1	3.50	1.80
H2	Malakoff, France	undetermined fish	tooth	limestone	platform		73.8	25.11	51.76
M3	Hallencourt, France	*Scapanorhynchus* sp.	tooth	limestone	offshore		82.1	0.92	0.57
D10	Sens, France	*Squalicorax pristodontus*	tooth	limestone	offshore		82.1	21.59	11.28
PI27	Somme, France	undetermined fish	tooth	limestone	upper offshore		87.4	11.03	7.01
D12	Beauval, France	undetermined fish	tooth	limestone	upper offshore		77.4	0.41	0.28
H6	Authon, France	undetermined fish	tooth	limestone	offshore		84.6	157.41	323.37
M2	Le Mans, France	*Squalicorax falcatus*	tooth	shales	upper offshore		94.5	14.28	22.79
PI23	Ardèche, France	undetermined fish	tooth	sandy limestone	upper offshore		91.2	40.35	86.60

Pr (ppm)	Nd (ppm)	Sm (ppm)	Eu (ppm)	Gd (ppm)	Tb (ppm)	Dy (ppm)	Ho (ppm)	Er (ppm)	Tm (ppm)	Yb (ppm)	Lu (ppm)	Σ(La + Sm + Yb)	(La/Sm) N	(Sm/Yb) N	Analytical method
47.12	190	36.53	8.37	48.56	7.10	41.40	8.78	22.30		12.72	1.64	217.25	0.67	1.46	ICP-MS
51.88	203	36.48	8.30	45.20	7.03	42.88	9.01	22.69		12.58	1.35	237.06	0.75	1.47	ICP-MS
60.81	267	61.14	12.26	71.64	9.68	50.93	9.98	23.76		12.58	1.71	256.72	0.43	2.47	ICP-MS
65.20	275	58.56	13.65	74.83	10.45	57.97	11.81	29.04		16.67	2.24	297.23	0.55	1.78	ICP-MS
87.13	377	82.36	18.74	102.00	14.20	78.26	15.74	38.85		22.68	2.97	404.04	0.53	1.85	ICP-MS
48.24	191	41.41	7.71	46.49	6.28	32.34	6.06	14.61		8.55	1.17	243.96	0.68	2.46	ICP-MS
20.44	85.40	16.73	4.01	22.41	3.25	19.05	4.08	10.53		6.9	0.9	111.13	0.76	1.23	ICP-MS
314	1533	378	64.56	315	33.70	150	24.12	46.03		21.41	3.03	4964.82	0.18	8.97	ICP-MS
171	739	174	27.32	133	14.45	57.51	8.93	18.42		9.53	1.39	2875.16	0.28	9.28	ICP-MS
17.58	75.50	15.50	3.30	17.18	2.38	13.00	2.64	6.78		4.47	0.61	86.97	0.63	1.76	ICP-MS
0.029	0.119	0.025	0.007	0.026	0.004	0.020	0.004	0.011		0.007	0.001	0.645	0.78	1.76	ICP-MS
0.024	0.109	0.022		0.026	0.004	0.022	0.005	0.012		0.008	0.001	0.560	0.63	1.33	ICP-MS
0.061	0.249	0.051		0.054	0.008	0.045	0.010	0.025		0.020	0.003	1.298	0.77	1.28	ICP-MS
0.052	0.225	0.050		0.066	0.010	0.068	0.016	0.040		0.031	0.005	1.226	0.82	0.82	ICP-MS
0.354	1.334	0.215		0.231	0.025	0.109	0.019	0.043		0.025	0.003	7.477	1.10	4.41	ICP-MS
0.38	1.51	0.23	0.06		0.04	0.33		0.25		0.20		3.92	2.21	0.60	ICP-MS
6.72	30.47	6.41	1.58		1.18	7.88		3.67		1.64		33.16	0.57	1.99	ICP-MS
0.11	0.43	0.06	0.02		0.01	0.09		0.06		0.04		1.02	2.20	0.77	ICP-MS
2.49	9.71	1.42	0.33		0.29	2.18		1.73		1.46		24.47	2.20	0.50	ICP-MS
1.77	7.26	1.18	0.27		0.19	1.21		0.64		0.31		12.52	1.36	1.92	ICP-MS
0.05	0.21	0.03	0.01		0.01	0.05		0.04		0.04		0.48	1.86	0.44	ICP-MS
71.72	317.72	62.51	15.32		9.11	55.04		26.67		10.71		230.63	0.37	2.97	ICP-MS
2.31	9.44	1.66	0.36		0.24	1.64		0.91		0.56		16.49	1.25	1.51	ICP-MS
9.01	36.99	6.87	1.66		0.98	5.48		2.84		1.79		49.01	0.85	1.95	ICP-MS

(continued on next page)

Table 2 (*continued*)

Samples	Location	Taxon	Material	Lithology	Environment	Period/stage	Proposed age (Ma)	La (ppm)	Ce (ppm)
This study									
M1	Les Renardières, France	*Carcharias amonensis*	tooth	sandy shales	upper offshore		94.5	7.59	18.06
D9	Yonne, France	*Lamna acuminata*	tooth	limestone	upper offshore		97.4	35.71	47.60
D5	Ardennes, France	*Odontaspis* sp.	tooth	green clays, phosphates	platform		105.5	25.15	84.21
D7	Courcelles, France	*Lamniform*	tooth	shales	upper offshore		105.6	262.72	533.56
PS25	La Houpette, France	*Otodus* sp.	tooth	sands, phosphorites	upper offshore		105.5	106.90	372.68
D2	Ardèche, France	*Otodus* sp.	tooth	shales	offshore		114.7	30.79	80.56
D3	Ardèche, France	*Pycnodus* sp.	tooth	shales	offshore		114.7	18.73	47.31
PI31	Ain, France	undetermined fish	tooth	limestone	platform		105.5	70.95	156.69
PI26	Viry, France	undetermined fish	tooth	unknown	shoreface		105.5	77.77	163.88
D4	Grusse, France	*Lamniform*	tooth	sandstone	shoreface		109.3		113.88
D6	Bellegarde, France	*Odontaspididae gracilis*	tooth	shales	upper offshore		120	79.27	165.69
D13	Martigues, France	undetermined fish	tooth	limestone	lower offshore		116.1	90.99	171.20
D1	Yonne, France	*Sphaerodus neocomiensis*	tooth	sandy limestone	upper offshore		129.5	16.81	41.47
V42	Auberson, Suisse	undetermined fish	tooth	limestone	upper offshore		134.8	255.18	948.68
V40	Bonvillars, Suisse	undetermined fish	tooth	limestone	offshore		137.5	94.66	564.92
V39	Ponte du Suchet, Suisse	undetermined fish	tooth	unknown	platform		136.2	396.39	1306.14
G2	Val de Fier, France	*Pycnodus* sp.	tooth	limestone	upper offshore		137	53.68	226.85
VSR	Gard, France	undetermined fish	tooth	limestone	offshore		136.75	6.43	40.30
G1	Ardèche, France	undetermined fish	tooth	shales	offshore		138.5	43.40	258.55
M4	Texas, USA	undetermined fish	tooth	unknown	platform		96.2	108.58	216.16
M5	Agadir, Morocco	*Squalicorax falcatus*	tooth	limestone	platform		91.25	44.29	54.09
M6	Texas, USA	undetermined fish	tooth	unknown	platform		88.5	72.01	101.84
Girard and Lecuyer (2002)									
K1-1	Kowala, Poland	*Palmatolepis*	conodont	limestone	distal platform	Frasnian	365	65.38	174.96
K1-2	Kowala, Poland	*Palmatolepis*	conodont	limestone	distal platform	Frasnian	365	63.43	175.02

Pr (ppm)	Nd (ppm)	Sm (ppm)	Eu (ppm)	Gd (ppm)	Tb (ppm)	Dy (ppm)	Ho (ppm)	Er (ppm)	Tm (ppm)	Yb (ppm)	Lu (ppm)	Σ(La + Sm + Yb)	(La/Sm) N	(Sm/Yb) N	Analytical method
2.10	9.89	2.10	0.50		0.29	1.64		0.67		0.42		10.11	0.53	2.55	ICP-MS
5.83	27.15	5.63	1.31		1.06	7.36		2.81		2.00		43.34	0.92	1.43	ICP-MS
6.74	27.55	5.90	1.45		0.99	5.98		3.29		2.23		33.28	0.62	1.35	ICP-MS
70.60	273.30	51.48	10.50		5.08	27.70		10.73		5.49		319.69	0.74	4.77	ICP-MS
23.91	82.31	14.85	3.27		1.80	8.76		2.83		1.80		123.55	1.05	4.19	ICP-MS
4.90	15.87	2.57	0.57		0.37	2.20		0.91		0.92		34.29	1.74	1.42	ICP-MS
4.71	24.92	5.52	1.33		0.91	5.21		2.44		1.53		25.79	0.49	1.83	ICP-MS
17.53	60.90	11.16	2.62		1.71	10.05		5.18		2.90		85.01	0.92	1.95	ICP-MS
16.19	62.20	12.05	2.84		2.02	12.72		6.50		4.50		94.32	0.94	1.36	ICP-MS
9.32	37.79	6.93	1.66		1.43	10.63		6.49		5.63		193.76		0.63	ICP-MS
17.12	80.99	14.07	3.18		2.35	15.06		7.81		5.26		98.61	0.82	1.36	ICP-MS
14.70	51.80	9.44	2.24		1.84	13.56		9.10		6.88		107.30	1.40	0.70	ICP-MS
4.02	14.53	2.76	0.63		0.45	2.93		1.53		1.14		20.71	0.89	1.22	ICP-MS
111.30	487.93	91.91	19.95		11.20	59.80		20.12		10.02		357.11	0.40	4.66	ICP-MS
37.01	150.63	33.20	7.86		4.51	25.29		8.76		3.78		131.64	0.41	4.46	ICP-MS
167.73	746.70	175.97	35.73		20.82	94.23		31.27		11.17		583.53	0.33	8.00	ICP-MS
23.13	104.96	23.19	4.81		2.37	10.09		3.14		1.26		78.13	0.34	9.36	ICP-MS
9.30	65.17	22.50	5.46		3.51	18.28		4.22		1.26		176.42	0.04	9.09	ICP-MS
55.02	383.82	135.79	33.95		20.09	99.72		24.72		7.27		1062.32	0.05	9.49	ICP-MS
21.13	84.29	13.45	2.78		1.84	11.66		5.28		3.52		125.55	1.17	1.94	ICP-MS
7.21	27.56	4.40	1.06		0.72	4.83		2.68		1.68		50.36	1.46	1.33	ICP-MS
9.81	38.60	6.46	1.46		1.21	9.14		5.81		5.40		83.87	1.62	0.61	ICP-MS
32.90	159.03	37.76	8.04	38.65	5.09	23.04		6.73		2.79		105.93	0.33	7.19	ICP-MS
32.36	147.48	34.09	7.07	33.34	4.34	19.24		6.24		2.71		100.23	0.35	6.69	ICP-MS

(continued on next page)

Table 2 (*continued*)

Samples	Location	Taxon	Material	Lithology	Environment	Period/stage	Proposed age (Ma)	La (ppm)	Ce (ppm)
Girard and Lecuyer (2002)									
K1-3	Kowala, Poland	*Palmatolepis*	conodont	limestone	distal platform	Frasnian	365	78.72	206.98
K1-4	Kowala, Poland	*Palmatolepis*	conodont	limestone	distal platform	Frasnian	365	35.38	88.46
K1-5	Kowala, Poland	*Palmatolepis*	conodont	limestone	distal platform	Frasnian	365	73.77	194.86
K4-1	Kowala, Poland	*Palmatolepis*	conodont	limestone	distal platform	Frasnian	365	57.96	123.48
K4-2	Kowala, Poland	*Palmatolepis*	conodont	limestone	distal platform	Frasnian	365	37.49	98.02
K4-3	Kowala, Poland	*Palmatolepis*	conodont	limestone	distal platform	Frasnian	365	58.91	141.50
K4-4	Kowala, Poland	*Palmatolepis*	conodont	limestone	distal platform	Frasnian	365	33.05	78.63
K4-5	Kowala, Poland	*Palmatolepis*	conodont	limestone	distal platform	Frasnian	365	27.68	68.99
K8-1	Kowala, Poland	*Palmatolepis*	conodont	limestone	distal platform	Frasnian	365	56.53	92.24
K8-2	Kowala, Poland	*Palmatolepis*	conodont	limestone	distal platform	Frasnian	365	61.86	99.24
K8-3	Kowala, Poland	*Palmatolepis*	conodont	limestone	distal platform	Frasnian	365	52.87	86.25
K8-4	Kowala, Poland	*Palmatolepis*	conodont	limestone	distal platform	Frasnian	365	58.58	94.48
K13-1	Kowala, Poland	*Palmatolepis*	conodont	limestone	distal platform	Frasnian	365	64.03	172.03
K13-2	Kowala, Poland	*Palmatolepis*	conodont	limestone	distal platform	Frasnian	365	58.60	146.29
K13-3	Kowala, Poland	*Palmatolepis*	conodont	limestone	distal platform	Frasnian	365	277.59	689.24
K13-4	Kowala, Poland	*Palmatolepis*	conodont	limestone	distal platform	Frasnian	365	108.74	253.79
K13-5	Kowala, Poland	*Palmatolepis*	conodont	limestone	distal platform	Frasnian	365	142.78	354.03
K15-1	Kowala, Poland	*Palmatolepis*	conodont	limestone	distal platform	Frasnian	365	238.56	549.37
K15-2	Kowala, Poland	*Palmatolepis*	conodont	limestone	distal platform	Frasnian	365	301.91	727.65
K15-3	Kowala, Poland	*Palmatolepis*	conodont	limestone	distal platform	Frasnian	365	220.56	535.97
K15-4	Kowala, Poland	*Palmatolepis*	conodont	limestone	distal platform	Frasnian	365	190.76	481.19
K15-5	Kowala, Poland	*Palmatolepis*	conodont	limestone	distal platform	Frasnian	365	194.91	484.35
K18-1	Kowala, Poland	*Palmatolepis*	conodont	limestone	distal platform	Frasnian	365	61.98	144.39
K18-2	Kowala, Poland	*Palmatolepis*	conodont	limestone	distal platform	Frasnian	365	113.37	274.74
K18-3	Kowala, Poland	*Palmatolepis*	conodont	limestone	distal platform	Frasnian	365	43.76	100.27

Pr (ppm)	Nd (ppm)	Sm (ppm)	Eu (ppm)	Gd (ppm)	Tb (ppm)	Dy (ppm)	Ho (ppm)	Er (ppm)	Tm (ppm)	Yb (ppm)	Lu (ppm)	Σ(La + Sm + Yb)	(La/Sm) N	(Sm/Yb) N	Analytical method
38.87	184.16	42.94	9.54	42.42	5.65	25.71		7.94		3.59		125.25	0.35	6.36	ICP-MS
16.49	77.91	18.82	4.00	19.73	2.64	11.95		3.69		1.36		55.56	0.36	7.37	ICP-MS
36.22	172.28	41.23	8.24	40.24	5.51	25.01		7.75		3.04		118.04	0.34	7.20	ICP-MS
23.16	108.21	25.62	5.62	26.92	3.71	18.34		6.79		3.73		87.31	0.43	3.65	ICP-MS
17.78	81.16	19.14	4.15	19.62	2.75	12.70		4.87		2.37		59	0.37	4.29	ICP-MS
26.07	122.94	28.45	6.42	29.46	4.04	19.42		6.43		2.61		89.97	0.39	5.78	ICP-MS
14.24	66.36	15.57	3.39	16.66	2.27	10.81		3.75		1.44		50.06	0.40	5.74	ICP-MS
12.78	59.83	13.78	3.05	13.80	1.93	9.23		2.92		1.08		42.54	0.38	6.80	ICP-MS
18.62	82.03	17.79	3.50	16.97	2.40	11.52		3.74		1.08		75.4	0.60	8.77	ICP-MS
20.08	90.07	19.62	4.03	20.60	2.79	13.74		4.63		1.86		83.34	0.60	5.62	ICP-MS
17.46	79.65	17.17	3.52	17.67	2.50	12.28		4.11		1.66		71.7	0.58	5.49	ICP-MS
18.95	85.37	18.53	3.71	18.60	2.60	12.51		4.56		1.69		78.8	0.60	5.83	ICP-MS
29.19	128.39	30.07	6.88	30.86	4.36	20.91		8.20		3.74		97.84	0.40	4.27	ICP-MS
24.57	108.02	24.52	5.45	23.69	3.32	16.15		5.26		1.98		85.1	0.45	6.59	ICP-MS
119.85	553.83	127.88	26.17	125.20	17.69	88.34		32.39		15.50		420.97	0.41	4.38	ICP-MS
45.00	206.24	47.03	10.72	48.17	6.81	33.11		12.28		5.33		161.1	0.44	4.69	ICP-MS
62.61	289.35	67.14	15.03	67.91	9.53	47.71		17.26		8.25		218.17	0.40	4.32	ICP-MS
96.43	442.31	97.71	20.20	98.41	13.54	64.03		22.39		9.68		345.95	0.46	5.36	ICP-MS
127.99	590.41	129.95	26.31	127.99	17.26	81.26		27.50		11.20		443.06	0.44	6.16	ICP-MS
93.11	430.19	93.63	19.81	91.69	12.52	58.87		19.95		8.06		322.25	0.44	6.17	ICP-MS
84.70	391.69	89.09	18.92	86.11	11.77	56.49		19.27		8.45		288.3	0.40	5.60	ICP-MS
84.56	385.76	84.22	18.14	81.80	11.01	52.35		17.13		6.95		286.08	0.44	6.43	ICP-MS
22.95	101.82	23.23	4.74	22.40	2.94	12.96		3.66		1.32		86.53	0.50	9.33	ICP-MS
44.25	196.16	44.21	9.06	41.79	5.47	24.24		7.39		2.85		160.43	0.48	8.25	ICP-MS
15.85	72.49	16.00	3.58	16.49	2.15	9.53		2.47		0.61		60.37	0.52	13.89	ICP-MS

(continued on next page)

Table 2 (*continued*)

Samples	Location	Taxon	Material	Lithology	Environment	Period/stage	Proposed age (Ma)	La (ppm)	Ce (ppm)
Girard and Lecuyer (2002)									
K18-4	Kowala, Poland	*Palmatolepis*	conodont	limestone	distal platform	Frasnian	365	248.90	563.82
K18-5	Kowala, Poland	*Palmatolepis*	conodont	limestone	distal platform	Frasnian	365	74.26	172.70
K23B-1	Kowala, Poland	*Palmatolepis*	conodont	limestone	distal platform	Frasnian	365	83.93	160.41
K23B-2	Kowala, Poland	*Palmatolepis*	conodont	limestone	distal platform	Frasnian	365	87.41	163.55
K23B-3	Kowala, Poland	*Palmatolepis*	conodont	limestone	distal platform	Frasnian	365	113.95	213.88
K23B-4	Kowala, Poland	*Palmatolepis*	conodont	limestone	distal platform	Frasnian	365	103.19	190.23
K23B-5	Kowala, Poland	*Palmatolepis*	conodont	limestone	distal platform	Frasnian	365	52.27	97.70
K24B1-1	Kowala, Poland	*Palmatolepis*	conodont	limestone	distal platform	Famennian	360	200.08	359.29
K24B1-2	Kowala, Poland	*Palmatolepis*	conodont	limestone	distal platform	Famennian	360	148.31	273.88
K24B1-3	Kowala, Poland	*Palmatolepis*	conodont	limestone	distal platform	Famennian	360	186.96	347.09
K24B1-4	Kowala, Poland	*Palmatolepis*	conodont	limestone	distal platform	Famennian	360	190.43	337.06
K24B1-5	Kowala, Poland	*Palmatolepis*	conodont	limestone	distal platform	Famennian	360	215.44	391.30
K24B2-1	Kowala, Poland	*Palmatolepis*	conodont	limestone	distal platform	Famennian	360	186.08	324.71
K24B2-2	Kowala, Poland	*Palmatolepis*	conodont	limestone	distal platform	Famennian	360	164.91	295.27
K24B2-3	Kowala, Poland	*Palmatolepis*	conodont	limestone	distal platform	Famennian	360	180.51	327.91
K24B2-4	Kowala, Poland	*Palmatolepis*	conodont	limestone	distal platform	Famennian	360	139.51	239.78
K24B2-5	Kowala, Poland	*Palmatolepis*	conodont	limestone	distal platform	Famennian	360	178.22	308.70
K24B3-1	Kowala, Poland	*Palmatolepis*	conodont	limestone	distal platform	Famennian	360	245.19	419.79
K24B3-2	Kowala, Poland	*Palmatolepis*	conodont	limestone	distal platform	Famennian	360	227.26	386.66
K24B3-3	Kowala, Poland	*Palmatolepis*	conodont	limestone	distal platform	Famennian	360	224.14	391.91
K24B3-4	Kowala, Poland	*Palmatolepis*	conodont	limestone	distal platform	Famennian	360	98.61	167.67
K24B3-5	Kowala, Poland	*Palmatolepis*	conodont	limestone	distal platform	Famennian	360	188.41	325.29
K25A-1	Kowala, Poland	*Palmatolepis*	conodont	limestone	distal platform	Famennian	360	31.57	54.84
K25A-2	Kowala, Poland	*Palmatolepis*	conodont	limestone	distal platform	Famennian	360	43.57	76.05
K25A-3	Kowala, Poland	*Palmatolepis*	conodont	limestone	distal platform	Famennian	360	100.18	163.74

Pr (ppm)	Nd (ppm)	Sm (ppm)	Eu (ppm)	Gd (ppm)	Tb (ppm)	Dy (ppm)	Ho (ppm)	Er (ppm)	Tm (ppm)	Yb (ppm)	Lu (ppm)	Σ(La + Sm + Yb)	(La/Sm) N	(Sm/Yb) N	Analytical method
90.21	414.84	92.83	19.16	95.00	12.47	58.86		19.31		8.71		350.44	0.51	5.66	ICP-MS
27.83	127.86	28.11	6.04	29.75	3.96	16.64		4.51		1.00		103.37	0.50	14.91	ICP-MS
26.83	122.53	26.10	6.24	29.13	3.93	18.91		6.69		2.07		112.1	0.61	6.70	ICP-MS
26.80	124.67	26.72	6.14	30.16	4.24	19.17		6.28		2.03		116.16	0.62	6.99	ICP-MS
36.04	166.37	35.12	8.30	40.21	5.24	25.14		9.30		3.95		153.02	0.61	4.73	ICP-MS
30.49	138.95	29.25	6.75	33.00	4.49	21.00		7.31		2.27		134.71	0.67	6.84	ICP-MS
16.22	74.40	15.82	3.76	18.40	2.62	12.15		4.45		1.80		69.89	0.62	4.67	ICP-MS
63.92	299.26	65.81	15.27	77.46	10.41	48.95		19.09		8.75		274.64	0.57	4.00	ICP-MS
45.11	211.31	46.74	11.38	54.41	7.39	37.06		14.40		6.76		201.81	0.60	3.67	ICP-MS
56.84	262.09	54.45	12.72	59.88	7.83	40.41		15.39		6.16		247.57	0.65	4.70	ICP-MS
58.85	282.28	60.90	14.68	73.72	9.64	48.01		18.33		8.63		259.96	0.59	3.75	ICP-MS
64.75	304.36	65.26	15.62	74.74	10.21	50.76		20.38		9.27		289.97	0.62	3.74	ICP-MS
68.25	334.12	77.02	18.20	87.30	11.90	59.82		22.59		10.12		273.22	0.46	4.04	ICP-MS
57.70	283.68	62.76	15.30	73.51	10.05	51.82		19.75		8.61		236.28	0.50	3.87	ICP-MS
64.80	314.02	70.25	17.44	80.70	11.36	53.70		20.70		9.66		260.42	0.49	3.86	ICP-MS
49.09	235.36	49.70	11.23	53.49	7.18	37.11		12.42		5.84		195.05	0.53	4.52	ICP-MS
62.54	311.15	69.84	16.58	81.26	11.27	55.17		21.11		9.70		257.76	0.48	3.82	ICP-MS
89.07	432.57	99.27	21.52	110.32	15.60	75.56		29.45		12.64		357.1	0.47	4.17	ICP-MS
83.20	401.43	89.89	21.70	109.68	15.96	75.17		27.70		13.99		331.14	0.48	3.41	ICP-MS
81.12	398.04	92.54	22.15	109.21	15.62	75.98		30.24		15.37		332.05	0.46	3.20	ICP-MS
35.85	180.33	42.30	9.93	52.20	7.25	34.65		13.68		5.86		146.77	0.44	3.83	ICP-MS
67.82	330.67	76.34	18.40	91.65	12.60	61.96		23.92		10.60		275.35	0.47	3.83	ICP-MS
11.14	54.58	12.81	2.91	15.25	2.11	10.18		3.52		1.32		45.7	0.47	5.16	ICP-MS
14.49	75.71	15.50	3.60	19.87	2.75	13.49		4.56		2.24		61.31	0.53	3.67	ICP-MS
34.15	161.22	36.58	7.94	40.61	5.69	28.46		11.14		4.29		141.05	0.52	4.53	ICP-MS

(continued on next page)

Table 2 (*continued*)

Samples	Location	Taxon	Material	Lithology	Environment	Period/stage	Proposed age (Ma)	La (ppm)	Ce (ppm)
Girard and Lecuyer (2002)									
K25A-4	Kowala, Poland	*Palmatolepis*	conodont	limestone	distal platform	Famennian	360	38.86	63.43
K25A-5	Kowala, Poland	*Palmatolepis*	conodont	limestone	distal platform	Famennian	360	120.28	194.89
K25B-1	Kowala, Poland	*Palmatolepis*	conodont	limestone	distal platform	Famennian	360	49.50	86.53
K25B-2	Kowala, Poland	*Palmatolepis*	conodont	limestone	distal platform	Famennian	360	92.27	157.26
K25B-3	Kowala, Poland	*Palmatolepis*	conodont	limestone	distal platform	Famennian	360	32.41	54.75
K25B-4	Kowala, Poland	*Palmatolepis*	conodont	limestone	distal platform	Famennian	360	50.13	86.40
K25B-5	Kowala, Poland	*Palmatolepis*	conodont	limestone	distal platform	Famennian	360	97.45	167.07
K25C-1	Kowala, Poland	*Palmatolepis*	conodont	limestone	distal platform	Famennian	360	44.05	76.98
K25C-2	Kowala, Poland	*Palmatolepis*	conodont	limestone	distal platform	Famennian	360	70.57	102.70
K25C-3	Kowala, Poland	*Palmatolepis*	conodont	limestone	distal platform	Famennian	360	116.43	197.76
K25C-4	Kowala, Poland	*Palmatolepis*	conodont	limestone	distal platform	Famennian	360	70.48	122.18
K25C-5	Kowala, Poland	*Palmatolepis*	conodont	limestone	distal platform	Famennian	360	53.58	95.01
K26B2-1	Kowala, Poland	*Palmatolepis*	conodont	limestone	distal platform	Famennian	360	145.83	266.13
K26B2-2	Kowala, Poland	*Palmatolepis*	conodont	limestone	distal platform	Famennian	360	232.21	389.11
K26B2-3	Kowala, Poland	*Palmatolepis*	conodont	limestone	distal platform	Famennian	360	400.86	764.56
K26B2-4	Kowala, Poland	*Palmatolepis*	conodont	limestone	distal platform	Famennian	360	318.56	602.91
K26B-5	Kowala, Poland	*Palmatolepis*	conodont	limestone	distal platform	Famennian	360	358.37	666.39
K28-1	Kowala, Poland	*Palmatolepis*	conodont	limestone	distal platform	Famennian	360	354.57	694.38
K28-2	Kowala, Poland	*Palmatolepis*	conodont	limestone	distal platform	Famennian	360	239.81	443.72
K28-3	Kowala, Poland	*Palmatolepis*	conodont	limestone	distal platform	Famennian	360	327.16	637.61
K28-4	Kowala, Poland	*Palmatolepis*	conodont	limestone	distal platform	Famennian	360	339.14	650.94
K28-5	Kowala, Poland	*Palmatolepis*	conodont	limestone	distal platform	Famennian	360	245.73	471.60
K31-1	Kowala, Poland	*Palmatolepis*	conodont	limestone	distal platform	Famennian	360	177.27	371.79
K31-2	Kowala, Poland	*Palmatolepis*	conodont	limestone	distal platform	Famennian	360	205.13	439.74
K31-3	Kowala, Poland	*Palmatolepis*	conodont	limestone	distal platform	Famennian	360	115.98	230.72

Pr (ppm)	Nd (ppm)	Sm (ppm)	Eu (ppm)	Gd (ppm)	Tb (ppm)	Dy (ppm)	Ho (ppm)	Er (ppm)	Tm (ppm)	Yb (ppm)	Lu (ppm)	Σ(La + Sm + Yb)	(La/Sm) N	(Sm/Yb) N	Analytical method
12.90	60.55	12.99	2.79	12.54	1.63	8.49		2.75		0.93		52.78	0.57	7.43	ICP-MS
41.08	205.54	45.47	10.72	56.81	7.97	38.21		14.62		6.74		172.49	0.50	3.58	ICP-MS
17.66	86.78	19.97	4.26	23.32	3.44	15.54		5.28		2.07		71.54	0.47	5.12	ICP-MS
33.21	162.14	36.06	8.83	43.68	6.04	28.55		10.66		4.97		133.3	0.48	3.85	ICP-MS
10.87	53.62	12.40	2.71	13.99	2.03	9.43		3.20		1.28		46.09	0.49	5.16	ICP-MS
17.73	85.72	19.99	4.47	23.32	3.31	15.05		5.43		2.02		72.14	0.47	5.25	ICP-MS
34.24	164.86	38.38	8.67	44.89	6.12	30.01		10.91		4.70		140.53	0.48	4.34	ICP-MS
15.32	77.64	16.71	3.71	20.46	3.10	12.95		4.45		2.05		62.81	0.50	4.33	ICP-MS
21.77	106.37	23.52	5.71	29.19	4.08	19.74		6.98		2.90		96.99	0.57	4.31	ICP-MS
40.44	196.81	44.14	10.55	53.49	7.50	35.33		12.84		5.47		166.04	0.50	4.28	ICP-MS
25.25	123.53	27.22	6.40	33.19	4.52	21.58		7.97		2.89		100.59	0.49	5.00	ICP-MS
19.37	96.72	22.20	4.90	27.39	3.88	17.63		6.04		2.68		78.46	0.46	4.40	ICP-MS
56.58	279.39	64.85	14.08	69.40	9.42	44.52		15.77		6.76		217.44	0.42	5.10	ICP-MS
84.73	429.34	100.51	22.25	116.46	15.58	75.68		29.92		13.47		346.19	0.44	3.96	ICP-MS
163.18	767.97	176.96	39.76	181.07	24.30	115.48		39.91		18.89		596.71	0.43	4.98	ICP-MS
131.93	644.47	148.81	32.93	157.92	21.18	101.74		36.35		16.15		483.52	0.40	4.89	ICP-MS
145.49	713.80	165.79	35.02	177.54	23.93	116.36		42.91		20.00		544.16	0.41	4.40	ICP-MS
155.54	756.42	176.07	39.21	179.54	24.30	115.11		39.33		18.47		549.11	0.38	5.06	ICP-MS
98.23	452.28	102.30	21.45	96.80	12.76	60.18		20.54		8.97		351.08	0.44	6.06	ICP-MS
142.04	693.60	159.65	33.70	164.79	21.82	102.53		34.40		15.09		501.9	0.39	5.62	ICP-MS
142.91	681.20	154.89	33.43	155.05	20.46	95.09		31.78		14.14		508.17	0.41	5.82	ICP-MS
103.90	487.45	109.77	23.57	105.06	13.89	63.94		21.51		9.30		364.8	0.42	6.27	ICP-MS
81.08	393.90	89.38	18.57	89.65	11.65	53.64		16.81		6.77		273.42	0.37	7.01	ICP-MS
93.78	439.40	98.53	20.36	90.51	11.75	52.44		15.89		5.87		309.53	0.39	8.91	ICP-MS
50.50	242.22	54.84	11.64	54.04	7.00	32.03		9.99		3.86		174.68	0.40	7.55	ICP-MS

(continued on next page)

Table 2 (*continued*)

Samples	Location	Taxon	Material	Lithology	Environment	Period/stage	Proposed age (Ma)	La (ppm)	Ce (ppm)
Girard and Lecuyer (2002)									
K31-4	Kowala, Poland	*Palmatolepis*	conodont	limestone	distal platform	Famennian	360	162.71	325.20
K35B-1	Kowala, Poland	*Palmatolepis*	conodont	limestone	distal platform	Famennian	360	46.57	81.58
K35B-2	Kowala, Poland	*Palmatolepis*	conodont	limestone	distal platform	Famennian	360	69.06	122.22
K35B-3	Kowala, Poland	*Palmatolepis*	conodont	limestone	distal platform	Famennian	360	50.25	88.51
K35B-4	Kowala, Poland	*Palmatolepis*	conodont	limestone	distal platform	Famennian	360	248.90	479.25
Wright et al. (1984)									
JWC56	Utah, USA	conodont, fish	not precised	Thaynes Fm	not precised	Smithian-Spathian	240	107	369
JWC54	Texas, USA	fish	not precised	Pinery Fm	not precised	Upper Guadalupian	265	202	158
JWC51	Ohio, USA	conodont	not precised	Ames Ls	not precised	Virgilian	295	43.8	89.8
JWC46	Ohio, USA	conodont	not precised	Ames Ls	not precised	Virgilian	295	48	83
JWC45	Ohio, USA	conodont	not precised	Portersville Ls	not precised	Upper Missourian	305	16.8	38.5
JWC41	Illinois, USA	conodont	not precised	Spoon Fm	not precised	Lower Desmoinesian	310	27.5	54
JWC52	Nevada, USA	conodont	not precised	Basal Riepe Springs	not precised	Lower Desmoinesian	310	64.8	29.5
JWC53	Nevada, USA	fish	not precised	Basal Riepe Springs	not precised	Lower Desmoinesian	310	970	436
JW4	Nevada, USA	conodont, fish	not precised	Basal Riepe Springs	not precised	Lower Desmoinesian	310	103	52
JWC43	Ohio, USA	conodont	not precised	L. Mercer Ls	not precised	Middle Atokan	320	22.9	50.8
JWC40	Texas, USA	conodont	not precised	Barnett Fm	not precised	Lower Chesterian	325	118	100
JW6_1	Lancashire, England	conodont	not precised	unknown	not precised	Mississippian	350	21.9	21.6
JWC39	Indiana, USA	conodont	not precised	New Albany Shale	not precised	Upper Kinderhookian	350	41.3	131
JWC38	Indiana, USA	conodont	not precised	New Albany Shale	not precised	Upper Kinderhookian	350	44	110
JWC37	Wyoming, USA	conodont	not precised	Lodgepole limestone	not precised	Middle Kinderhookian	350	104	93
JWC36	Missouri, USA	conodont	not precised	Bushberg sandstone	not precised	Middle Kinderhookian	350	77.9	159
JWC35	Wyoming, USA	conodont	not precised	Madison limestone	not precised	Middle Kinderhookian	350	124	228
JWC5_1	Missouri, USA	conodont	not precised	Holt summit sandstone	not precised	Famennian	360	84.1	205
JWC33	Nevada, USA	conodont	not precised	Pilot shale	not precised	Famennian	360	104	261

Pr (ppm)	Nd (ppm)	Sm (ppm)	Eu (ppm)	Gd (ppm)	Tb (ppm)	Dy (ppm)	Ho (ppm)	Er (ppm)	Tm (ppm)	Yb (ppm)	Lu (ppm)	Σ(La + Sm + Yb)	(La/Sm) N	(Sm/Yb) N	Analytical method
70.05	335.58	76.27	16.53	76.83	9.71	45.99		14.56		5.32		244.3	0.40	7.62	ICP-MS
16.61	76.55	16.69	3.54	17.50	2.33	11.36		3.56		1.30		64.56	0.53	6.82	ICP-MS
24.50	112.61	24.63	5.08	25.93	3.52	17.16		5.60		2.16		95.85	0.53	6.05	ICP-MS
17.68	82.47	18.01	3.70	19.08	2.58	12.96		4.28		1.41		69.67	0.53	6.77	ICP-MS
101.13	480.98	106.15	23.36	107.62	14.03	65.04		21.41		8.08		363.13	0.44	6.98	ICP-MS
	178	33.1	5.9		4.4					3.9	0.35	144	0.58	4.62	Neutron activation
	181	54.8	8.6		7.8					8.8	0.95	265.6	0.66	3.39	Neutron activation
	50	15.4	3.63		2.34					2.81	0.41	62.01	0.51	2.98	Neutron activation
	90	19	3.89							4.4	0.43	71.4	0.45	2.35	Neutron activation
		7.68	2		1.03					1.57	0.22	26.05	0.39	2.66	Neutron activation
	60	9.5	3.2		1.68					2		39	0.52	2.58	Neutron activation
	24	9.7	5.09		1.1					2.1	0.18	76.6	1.19	2.51	Neutron activation
	600	117.4	29.4		12.3					47	37	1134.4	1.47	1.36	Neutron activation
		14.4	6.5		2.2					3.9	0.56	121.3	1.27	2.01	Neutron activation
	33	10	1.01		0.83					1.56	0.17	34.46	0.41	3.49	Neutron activation
	108	21.4	3.24		2.6					4.4	0.4	143.8	0.98	2.65	Neutron activation
	16	11.45	1.17		0.67					1		34.35	0.34	6.23	Neutron activation
	211	41.1	14.6		7.2					5	0.43	87.4	0.18	4.47	Neutron activation
	143	88	10.8		3					5.6		137.6	0.09	8.55	Neutron activation
	160	9			3.7					3.6		116.6	2.06	1.36	Neutron activation
	97	19.5	4.16		2.78					3.63	0.35	101.03	0.71	2.92	Neutron activation
	168	35.8	6.2		4.1					3.8	0.63	163.6	0.62	5.12	Neutron activation
	90	24.7	7.5		5.1					4.1	0.46	112.9	0.61	3.28	Neutron activation
	170	27	8.8		4.5					5.6		136.6	0.69	2.62	Neutron activation

(continued on next page)

Table 2 (*continued*)

Samples	Location	Taxon	Material	Lithology	Environment	Period/stage	Proposed age (Ma)	La (ppm)	Ce (ppm)
Wright et al. (1984)									
JWC32	Nevada, USA	conodont	not precised	Devil's gate limestone	not precised	Frasnian	367	108	142
JWC30	New York, USA	conodont	not precised	Genesee Fm	not precised	Frasnian	367	31.1	124
JWC28	Indiana, USA	conodont	not precised	New Albany shale	not precised	Givetian	375	35.3	72.3
JWC27	Ohio, USA	conodont	not precised	Deleware limestone	not precised	Eifelian	385	55.9	70.9
JWC26	Ohio, USA	conodont	not precised	Deleware limestone	not precised	Eifelian	385	85.4	92
JWC25	Ohio, USA	conodont	not precised	Columbus limestone	not precised	Eifelian	385	95	103
JWC23	Sunny Hill quarry, England	conodont	not precised	Upper Bringewood Fm	not precised	Upper Ludlovian	420	139	331
JWC4_1	England	conodont	not precised	unknown	not precised	Wenlockian	425	160	513
JW8	California, USA	conodont	not precised	Hidden valley dolomite	not precised	Wenlockian	425	179	373
JWC22	Kentucky, USA	conodont	not precised	Brassfield Fm	not precised	Llandoverian	435	137	370
JWC21	Ohio, USA	conodont	not precised	Brassfield Fm	not precised	Llandoverian	435	179	594
JWC20	Kentucky, USA	conodont	not precised	Ashlock Fm	not precised	Lower Ashgillian	445	57.4	118
JWC19	Kentucky, USA	conodont	not precised	Ashlock Fm	not precised	Lower Ashgillian	445	56.5	102
JWC17	Oklahoma, USA	conodont, fish	not precised	Corbin Ranch Fm	not precised	Lower Caradocian	455	54.2	61.6
JWC16	Oklahoma, USA	conodont	not precised	Tulip Crk. Fm	not precised	Llandeilian	464	90	352
JWC3_16	Öland, Sweden	conodont	not precised	unknown	not precised	Llanvirnian	467	66	182
JWC15	Oklahoma, USA	conodont	not precised	McLish Fm	not precised	Llanvirnian	467	25	78
JWC14	Oklahoma, USA	conodont	not precised	Joins Fm	not precised	Llanvirnian	467	76.8	387
JWC3_34	Oklahoma, USA	conodont	not precised	Signal Mtn Fm	not precised	Tremadocian	487	102.6	274
JWC3_24	Texas, USA	conodont	not precised	Wilbern Fm	not precised	Tremadocian	487	156	479
JW7	Nevada, USA	conodont	not precised	Dunderberg shale	not precised	Dresbachian	495	501	1200
Felitsyn et al. (1998)									
Ma-U1	Estonia/Russia	brachiopod	shell	sandstones	littoral	Middle Cambrian	504	116	270
T_3/28	Estonia/Russia	brachiopod	shell	sandstones	littoral	Late Cambrian	491	172	577
E_10/2	Estonia/Russia	unidentified	unidentified	unidentified	littoral	Late Cambrian	493	160	414

Pr (ppm)	Nd (ppm)	Sm (ppm)	Eu (ppm)	Gd (ppm)	Tb (ppm)	Dy (ppm)	Ho (ppm)	Er (ppm)	Tm (ppm)	Yb (ppm)	Lu (ppm)	Σ(La + Sm + Yb)	(La/Sm) N	(Sm/Yb) N	Analytical method
	97	20	3.67		2.4					3.6	0.27	131.6	0.96	3.02	Neutron activation
	153	54.3	13.9		7.7					2.58	0.238	87.98	0.10	11.45	Neutron activation
	53	15.6	4.09		3.4					3.53	0.36	54.43	0.40	2.40	Neutron activation
	73	16.6	4.58		3.3					2.07	0.266	74.57	0.60	4.36	Neutron activation
	103	25.8	6.44		4.6					4.5	0.41	115.7	0.59	3.12	Neutron activation
	170	39	5.53		3.3					4	0.25	138	0.43	5.30	Neutron activation
	300	78.3	15.4		8					6.6	0.42	223.9	0.32	6.45	Neutron activation
	360	122	22.1		15.4					11.8	0.98	293.8	0.23	5.62	Neutron activation
	604	60	6.2		5.8					2.6	0.38	241.6	0.53	12.55	Neutron activation
	430	100	24		9					12.8	0.9	249.8	0.24	4.25	Neutron activation
	423	93	21.3		16.2					9.7	0.84	281.7	0.34	5.21	Neutron activation
	52	9.67	2.76		2.01					1.8	0.17	68.87	1.06	2.92	Neutron activation
		11.3	2.2		1.8					1.9		69.7	0.89	3.23	Neutron activation
	22	6.95	1.33		0.85					2.53	0.2	63.68	1.39	1.49	Neutron activation
	250	82	12.4		6.5					7.4	0.57	179.4	0.20	6.03	Neutron activation
	110	63	8.1		5.4					3.4	0.25	132.4	0.19	10.08	Neutron activation
	100	5.7	5.2		2.3					4		34.7	0.78	0.78	Neutron activation
	421	91	16.6		8.6					2.1	0.24	169.9	0.15	23.57	Neutron activation
	180	47	6.7		2.8					3.2		152.8	0.39	7.99	Neutron activation
	180	120	9.5		6.3					5.9	0.51	281.9	0.23	11.06	Neutron activation
		197	17.5		24					11.4	1.38	709.4	0.45	9.40	Neutron activation
	140	30	7.9		6.5		8			10.4		156.4	0.69	1.57	Neutron activation
	401	73	14.6		11.9		10.5			14		259	0.42	2.84	Neutron activation
	260	47	10.3		9		10			13.6		220.6	0.61	1.88	Neutron activation

(continued on next page)

Table 2 (*continued*)

Samples	Location	Taxon	Material	Lithology	Environment	Period/stage	Proposed age (Ma)	La (ppm)	Ce (ppm)
Felitsyn et al. (1998)									
Syas_1	Estonia/Russia	brachiopod	shell	sandstones	littoral	Late Cambrian	491	210	660
Lava_1	Estonia/Russia	brachiopod	shell	sandstones	littoral	Late Cambrian	491	241	760
U_83_6	Estonia/Russia	brachiopod	shell	sandstones	littoral	Late Cambrian	491	158	397
U_83_8/9	Estonia/Russia	brachiopod	shell	sandstones	littoral	Early Ordovician	489	165	456
MBIbeta	Estonia/Russia	unidentified	conodont	limestones	littoral	Early Ordovician	481	367	1298
Tonu_5	Estonia/Russia	brachiopod	shell	limestones	littoral	Early Ordovician	476	701	1722
Tonu_24	Estonia/Russia	brachiopod	shell	limestones	littoral	Early Ordovician	474	586	1425
EST_1	Estonia/Russia	unidentified	unidentified	unidentified	littoral	Middle Ordovician	470	519	1559
EST_2	Estonia/Russia	unidentified	unidentified	unidentified	littoral	Middle Ordovician	470	681	1671
EST_3	Estonia/Russia	unidentified	unidentified	unidentified	littoral	Middle Ordovician	470	393	842
Shields and Stille (2001)									
SSF1	Tayshir, West Mongolia	unidentified	shelly fossil	dolomitic phosphorite	not precised	Lower Cambrian	530	209.4	357.6
SSF2	Tayshir, West Mongolia	unidentified	shelly fossil	dolomitic phosphorite	not precised	Lower Cambrian	530	242.3	386.8
SSF3_1	Tayshir, West Mongolia	unidentified	shelly fossil	dolomitic phosphorite	not precised	Lower Cambrian	530	152.9	168.9
SSF3_2	Tayshir, West Mongolia	unidentified	shelly fossil	dolomitic phosphorite	not precised	Lower Cambrian	530	150.4	251.8

Data have been compiled from Bertram et al. (1992), Elderfield and Pagett (1986), Felitsyn et al. (1998), Girard and Lécuyer (2002), Grandjean (1989), Grandjean et al. (1987, 1988), Kemp and Trueman (2003), Lécuyer et al. (1998, 2002), Picard et al. (2002), Shields and Stille (2001) and Wright et al. (1984).

$(Sm/Yb)_N$ ratios in Fig. 3a. For samples younger than 80 Ma, most $(Sm/Yb)_N$ ratios fall within the modern fresh and oceanic water range (only three outliers over more than 50 samples), and can thus be explained by various mixtures of shoreface and offshore components. $(Sm/Yb)_N$ ratios of samples older than 110 Ma fall above the modern seawater range. Such values are characteristic of old seawaters, for instance, in the Jurassic (Picard et al., 2002). Note that this observation would still hold if taking altered samples into account, as they show the highest $(Sm/Yb)_N$ ratios.

The major change in $(Sm/Yb)_N$ ratios of biogenic phosphates occurred progressively during the Cretaceous (Fig. 4a). This change is concurrent with a progressive decrease of the Ce anomaly (Fig. 4b) from positive values to negative values comparable to those observed in modern oceans (Elderfield and Greaves, 1982; De Baar et al., 1985; Elderfield, 1988; Alibo and Nozaki, 1999).

4. Discussion

4.1. REE contents: seawater composition or alteration signature?

The observed changes in REE patterns over time may either reflect seawater compositional changes

Pr (ppm)	Nd (ppm)	Sm (ppm)	Eu (ppm)	Gd (ppm)	Tb (ppm)	Dy (ppm)	Ho (ppm)	Er (ppm)	Tm (ppm)	Yb (ppm)	Lu (ppm)	Σ(La + Sm + Yb)	(La/Sm) N	(Sm/Yb) N	Analytical method
	351	63	16.7		11		12			17.6		290.6	0.59	1.95	Neutron activation
	330	76	19.7		13		17			23.6		340.6	0.56	1.75	Neutron activation
	238	43	10.8		9.2		11			14.2		215.2	0.65	1.65	Neutron activation
	260	48	13.2		9.9		12.2			15.4		228.4	0.61	1.70	Neutron activation
	795	148	30.8		21		18.8			25.4		540.4	0.44	3.17	Neutron activation
	1368	264	54.2		36		35.1			46.1		1011.1	0.47	3.11	Neutron activation
	1089	198	40.7		27		29.5			43.6		827.6	0.53	2.47	Neutron activation
	864	195	44	198	31					31	3	745	0.47	3.42	Neutron activation
	1225	256	58	258	38.6					34.4	3.4	971.4	0.47	4.05	Neutron activation
	664	128	28	126	26.6					27.1	3.2	548.1	0.55	2.57	Neutron activation
50.66	221.3	47.3	10.97	49.1	5.851	28.86	5.117	12.02	1.253	6.1	0.777	262.8	0.79	4.22	ICP-MS
52.67	236.9	50.7	11.63	54.88	6.334	30.84	5.442	12.53	1.233	6	0.785	299	0.85	4.60	ICP-MS
33.3	146.3	30.8	6.985	32.3	3.691	17.75	3.154	7.311	0.592	3.7	0.489	187.4	0.88	4.53	ICP-MS
33.32	146.7	30.9	7.104	33.59	3.843	19.48	3.343	8.072	0.871	4.43	0.579	185.73	0.87	3.79	ICP-MS

(Wright et al., 1984; Grandjean et al., 1987; Grandjean-Lécuyer et al., 1993) or various diagenetic processes such as:

- REE contributions from host sediments linked to lithological variations or;
- progressive alteration of REE contents with increasing geological age.

The REE budget of biogenic phosphates depends on contributions from both sediment pore waters and overlying water column (Elderfield and Pagett, 1986). Therefore, variations in host lithology of marine biogenic phosphates may influence their REE contents due to differences in permeability, REE composition, organic and oxide–hydroxide contents. To test this hypothesis, lithologies have been identified on the $(Sm/Yb)_N$ versus age plot (Fig. 3b). The REE contents of biogenic phosphates deposited in clays (6% of the database) are influenced by REE derived from the detrital flux which has a shale-like signal flat REE pattern (Grandjean et al., 1987), yielding $(Sm/Yb)_N$ ratios close to 1 (Fig. 3b). Samples from limestones and phosporites are deposited in domains that are relatively well protected from detrital influence and show the largest variations in their $(Sm/Yb)_N$ ratios. Biochemical sediments that precipitated directly from seawater have REE patterns reflecting the composi-

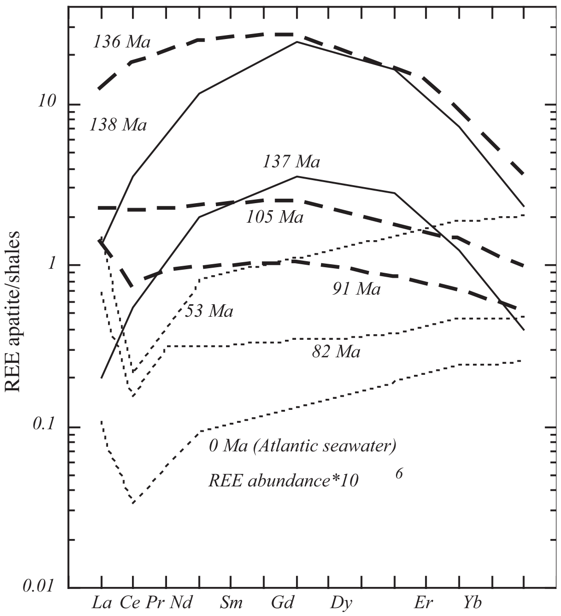

Fig. 1. Examples of the three main types of REE patterns recorded in our collection of analyzed Cretaceous marine biogenic apatites (Table 1). (1) "Bell-shaped" patterns of two recrystallized shark teeth from the Lower Cretaceous (137 and 138 Ma); (2) pre-Turonian fish teeth represented by thick streaked lines and characterized by no or weak negative Ce anomalies and HREE depletion relatively to LREE; (3) post-Turonian fish teeth and modern Atlantic seawater (De Baar et al., 1985) represented by thin dotted lines showing strong negative Ce anomalies and increasing REE abundance with atomic number. Fish tooth of Ypresian age (53 Ma) was sampled from northern Morocco phosphorite deposits (Grandjean et al., 1988).

tion of the overlying water column. This property of marine carbonates has been demonstrated by Elderfield et al. (1981) who measured REE patterns of foraminifer skeletons that reproduce those of surrounding marine waters. Similarly, biogenic apatites have been shown to acquire seawater-like REE patterns during early diagenesis close to water–sediment interface (Elderfield and Pagett, 1986). We must emphasize that our database includes mainly samples from carbonate and carbonate–phosporite deposits (65% of the database) (Fig. 3b). Samples from sandstones (about 10% of the database) have an intermediate pattern (e.g. Grandjean et al., 1987; Felyitsin et al., 1998), some similar to limestones, other similar to clays. Except for clays and clayey sandstones, we consider that the REE composition of biogenic phosphates from various lithologies reflect the REE composition of seawater.

Diagenesis following deposition can alter the absolute and relative abundance of the REE in biogenetic apatites. This is observed in samples exhibiting bell-shaped patterns characteristic of extensive diagenesis (Reynard et al., 1999). Interestingly, these patterns are observed in ancient (e.g. Devonian) as well as relatively recent (e.g. Cretaceous) samples, implying that this phenomenon is not dependent on age and results from specific events such as low grade metamorphic overprint and/or extensive dissolution–recrystallization. This is not the case for the $(Sm/Yb)_N$ ratios which are observed in the 110–540 Ma period. This could be attributed to a progressive low temperature alteration. In this latter case, systematic changes in the sum of REE could be expected but no such trend is observed with increasing age (Fig. 5). We only observe contents below 10 ppm in samples younger than 160 Ma.

The absence of significant correlation between the $(Sm/Yb)_N$ ratio and sum of the three selected REE (La + Sm + Yb) over the whole sample set (Fig. 6a) confirms that if any alteration occurred, it did not affect significantly the REE contents. Variations of the $(Sm/Yb)_N$ ratio and total REE content can be correlated with bathymetry when subsets from Elderfield and Pagett (1986) on contemporary fish remains and Picard et al. (2002) on Jurassic fish and reptile remains are considered (Fig. 6b). In contemporary samples, this correlation is due to REE fractionation in the water column; both the REE content and $(Sm/Yb)_N$ ratio decrease with increasing bathymetry. In contrast, Jurassic samples show a positive correlation between $(Sm/Yb)_N$ (and to a smaller extent the sum of REE) and palaeobathymetry. This is due to relative depletion of Yb and Lu in the water column demonstrated by Picard et al. (2002), and is consistent with estimation of bathymetry made from thermocline reconstruction with oxygen isotope studies on brachiopods (Picard et al., 1998). Part of the vertical scattering may be explained by variations in REE concentration between parts of fish remains such as tooth enamel and dentine (e.g. Picard et al., 2002). The homogeneity of REE patterns in different tissues (Grandjean and Albarède, 1989) further suggests the robustness of the REE record. Finally, progressive alteration over time would produce a smooth variation

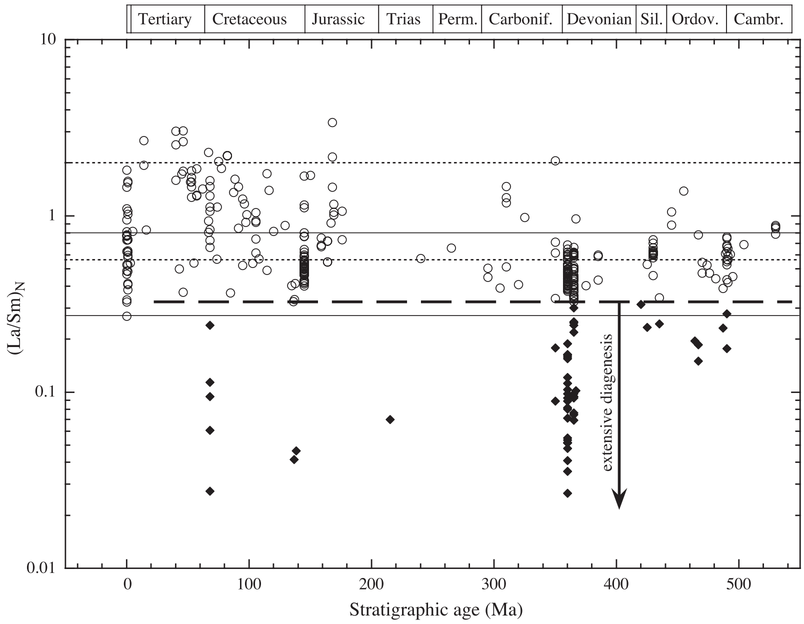

Fig. 2. Variations of $(La/Sm)_N$ ratios of marine biogenic phosphates (fish teeth, conodonts, lingulid shells) as a function of geological times (data from Table 2). Samples represented by diamonds fulfill the criterion of extensive diagenesis leading to strongly fractionated "bell-shaped" REE patterns with $(La/Sm)_N < 0.3$.

of the $(Sm/Yb)_N$ ratios, while the change between modern and ancient REE patterns are observed to occur over a limited time span (80–110 Ma), when compared with the stable high $(Sm/Yb)_N$ ratio over the 110–550 Ma interval and stable low $(Sm/Yb)_N$ ratio from 80 Ma to present. Thus, we attribute the change in REE patterns between 110 and 80 Ma to a change in seawater REE composition rather than to a change in the REE uptake mechanism in biogenic apatites.

4.2. Possible causes for a change in REE seawater composition

Having shown that the REE patterns of most samples can be reasonably associated to palaeoenvironmental factors and may thus be interpreted as reflecting the REE pattern of seawater at the time of deposition, we explore possible explanations for changes in REE seawater composition throughout geological times. In present-day seawater, dissolved REE contents increase from Sm to Yb: this pattern is attributed to scavenging of REE by organic or inorganic primary carriers (Elderfield and Greaves, 1982; Fowler et al., 1987). The REE compositional changes revealed in this study may therefore be due to concurrent changes in the composition and abundance of primary REE carriers throughout the Phanerozoic as previously suggested by Grandjean-Lécuyer et al. (1993). From Cambrian to Lower Cretaceous, the $(Sm/Yb)_N$ ratio of biogenic apatites from the Tethyan ocean ranges from 1 to 10, while "modern" seawater, younger than 80 Ma, is characterized by $(Sm/Yb)_N$ ratios generally lower than 1. This observation suggests that an efficient HREE removal or scavenging process existed in pre-Cretaceous seawater (Picard et al., 2002). To our knowledge, there is no present-day marine environment with such a strong relative depletion of the heaviest REE. Change in planktonic biomass or of physico-chemical properties such as redox conditions in seawater could have been responsible for a change in the REE seawater composition reflected by that of fossil biogenic apatites. However, we cannot propose any definitive explanation for the REE patterns of marine biogenic phosphates older than 110 Ma.

The amplitude of the Ce anomaly recorded in marine fish debris has been considered as a proxy

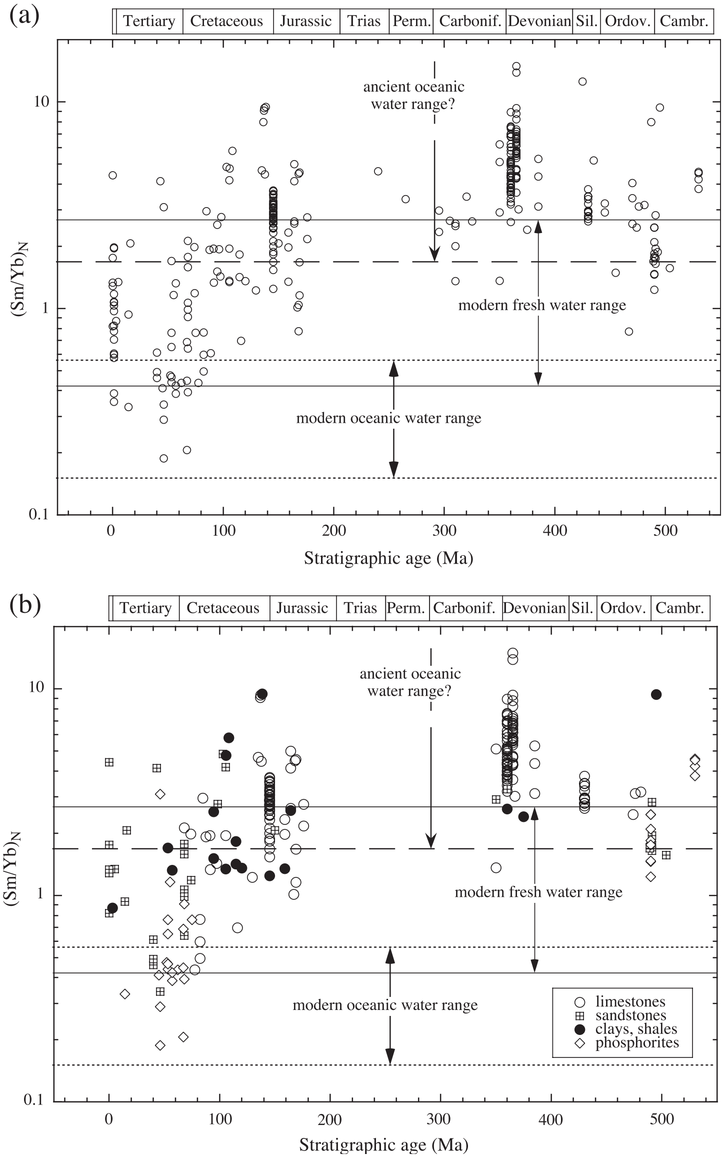

Fig. 3. Variations of $(Sm/Yb)_N$ ratios of marine biogenic phosphates (fish teeth, conodonts, lingulid shells) as a function of geological time (data from Table 2, filtered for extensive diagenesis according to Fig. 2): (a) all unaltered samples; (b) subset (host sediment known) of biogenic apatites from limestones, sandstones, shales and phosphorites.

of paleo-oceanic redox conditions (Wright et al., 1984, 1987; Liu et al., 1988). The proxy is based on the progressive oxidation of Ce^{3+} to Ce^{4+} with increasing seawater oxygenation; insoluble Ce^{4+} is readily incorporated into metal-oxide coatings (Piper, 1974; Elderfield et al., 1981; Elderfield, 1988; De Baar et al., 1988). An increase of dissolved oxygen in surface seawater could have been favored by cooler sea surface temperature, wind intensification, and enhanced oceanic stirring. The observed correlation between $(Sm/Yb)_N$ ratio and Ce anomaly of Cretaceous fish teeth, as shown in Fig. 4, supports the hypothesis of a progressive change in dynamics and chemistry of the Tethyan

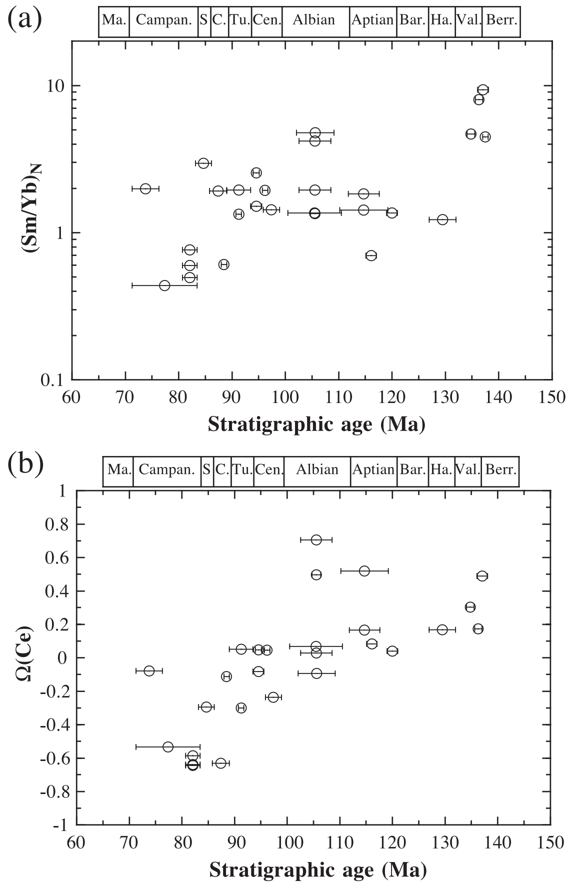

Fig. 4. Evolution of REE seawater chemistry through the Cretaceous as recorded in marine biogenic apatites from the Tethyan open marine platform environments (data from Table 1). Decreasing of $(Sm/Yb)_N$ ratios (a) are correlated with increasing negative Ce anomalies (b). This observation is interpreted as a progressive oxygenation of seawater resulting from major oceanographic changes consequently to the opening of the Atlantic ocean.

and proto-Atlantic waters between 110 and 80 Ma. On the basis of these observations, we propose that water masses evolved from stratified and poorly oxygenated surface seawaters prior to 110 Ma towards well-mixed and oxygenated waters at present. This major change in oceanic circulation could result from the contemporaneous opening of the Southern Atlantic Ocean (Scotese et al., 1988). Increased stirring, mixing, and oxygenation of water is potentially driven by new circulation patterns resulting from palaeogeography changes between Albian (≈ 110 Ma) and Turonian times (≈ 80 Ma) (Poulsen et al., 2001). This conclusion was also reached by Stille et al. (1996) from Nd isotopic compositions of Tethyan carbonates and phosphate concretions, fixing the period of circulation change around 80 Ma. We cannot also exclude that increasing oxygenation of surface waters was enhanced by global cooling after the Cenomanian/Turonian boundary as suggested by the increase of oxygen isotope compositions of both foraminifera (Saito and Van Donk, 1974; Huber et al., 1995; Frakes, 1999) and fish remains (Kolodny and Raab, 1988; Lécuyer et al., 1993). Finally, the overall modification of oceanic circulation may have modified the distribution of nutrients in the water column. This could constitute the main extrinsic parameter at the origin of the progressive colonization by the calcareous plankton of pelagic environments during the Middle and Late Cretaceous (Tappan and Loeblich, 1973; Bralower and Thierstein, 1984; Bolli et al., 1985; Roth, 1986).

5. Conclusion

Compilation of a database of biogenic apatite REE contents from the Phanerozoic and new data acquired on Cretaceous biogenic apatites from the Tethyan domain show that the REE patterns have changed through time. These data reveal a change in the relative REE compositions in Tethyan seawater between 110 and 80 Ma. At the end of the Cretaceous, the REE chemistry of seawater is constant until present-day. Prior to 110 Ma, REE patterns are all different from those of present-day seawater, although many of the analyzed samples come from open marine sedimentary environments. This is tentatively attributed to a change in the scavenging mechanism of REE in the water column.

In the 110–80 Ma period, changes in the mechanism of REE scavenging within the water column is marked by the decrease of $(Sm/Yb)_N$ ratio and the increase of Ce anomalies (ΩCe) that could reflect an evolution from stratified and poorly oxygenated waters towards well-mixed and oxygenated waters. This change is proposed to result from the coeval opening of the Atlantic ocean.

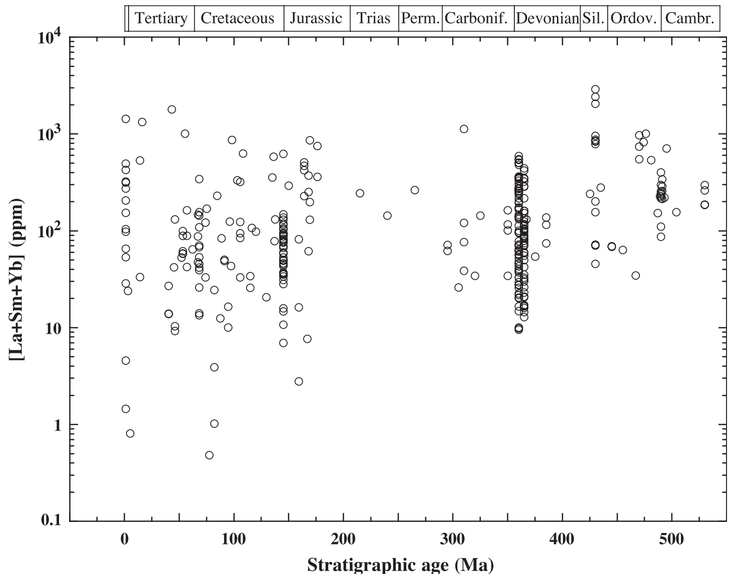

Fig. 5. Variations of the sum of the three selected REE (La + Sm + Yb) with age (data from Table 2). Only La, Sm and Yb are used because they are light, middle and heavy REE, respectively, and they represent adequately the pattern shape and are the most commonly analyzed REE in Table 2. Note that, apart from low concentration samples (sum < 10 ppm) occurring only in some samples younger than 160 Ma, the variation range has not significantly changed with time. Symbols as for Fig. 2.

Acknowledgements

The authors are grateful to F. Cordey who edited the English of this manuscript. E. H. Oelkers, B. Schmitz and D. Kidder are thanked for their constructive reviews that helped to improve the scientific content of this work. This study was supported by the French CNRS Program 'ECLIPSE'. **[EO]**

References

Alibo, D.S., Nozaki, Y., 1999. Rare earth elements in seawater: particle association, shale-normalization, and Ce oxidation. Geochim. Cosmochim. Acta 63, 363–372.

Aplin, A.C., 1984. Rare earth element geochemistry of central Pacific ferromanganese encrustations. Earth Planet. Sci. Lett. 71, 13–22.

Bernat, M., 1975. Les isotopes de l'uranium et du thorium et les terres rares dans l'environnement marin. Cah.-ORSTOM, Ser. Geol. 7, 68–83.

Bertram, C.J., Elderfield, H., Aldridge, R.J., Conway Morris, S., 1992. $^{87}Sr/^{86}Sr$, $^{143}Nd/^{144}Nd$ and REEs in Silurian phosphatic fossils. Earth Planet. Sci. Lett. 113, 239–249.

Bolli, H.M., Saunders, J.B., Perch-Nielsen, K., 1985. Plankton Stratigraphy. Cambridge Univ. Press, Cambridge.

Boyle, E.A., Edmond, J.M., Sholkovitz, E.R., 1977. The mechanism of iron removal in estuaries. Geochim. Cosmochim. Acta 41, 1313–1324.

Bralower, T.J., Thierstein, H.R., 1984. Low productivity and slow deep-water circulation in mid-Creteceous oceans. Geology 12, 614–618.

De Baar, H.J.W., Bacon, M.P., Brewer, P.G., 1985. Rare earth elements in the Pacific and Atlantic oceans. Geochim. Cosmochim. Acta 49, 1943–1959.

De Baar, H.J.W., German, C.R., Elderfield, H., Van Gaans, P., 1988. Rare earth element distributions in anoxic waters of the Cariaco Trench. Geochim. Cosmochim. Acta 52, 1203–1219.

Elderfield, H., 1988. The oceanic chemistry of the rare-earth elements. Philos. Trans. R. Soc. Lond. 325, 105–126.

Elderfield, H., Greaves, M.J., 1982. The rare earth elements in seawater. Nature 296, 214–219.

Elderfield, H., Pagett, R., 1986. Rare Earth elements in Ichthyoliths: variations with redox conditions and depositional environment. In: Riley, J.P. (Ed.), Sciences of the Total Environment, 49, 175–197.

Elderfield, H., Sholkovitz, E.R., 1987. Rare earth elements in porewater of reducing nearshore sediments. Earth Planet. Sci. Lett. 82, 280–288.

Elderfield, H., Hawkesworth, C.J., Greaves, M.J., Calvert, S.E., 1981. Rare earth element geochemistry of oceanic ferromanganese nodules and associated sediments. Geochim. Cosmochim. Acta 45, 513–528.

Felitsyn, S., Sturesson, U., Popov, L., Holmer, L., 1998. Nd isotope

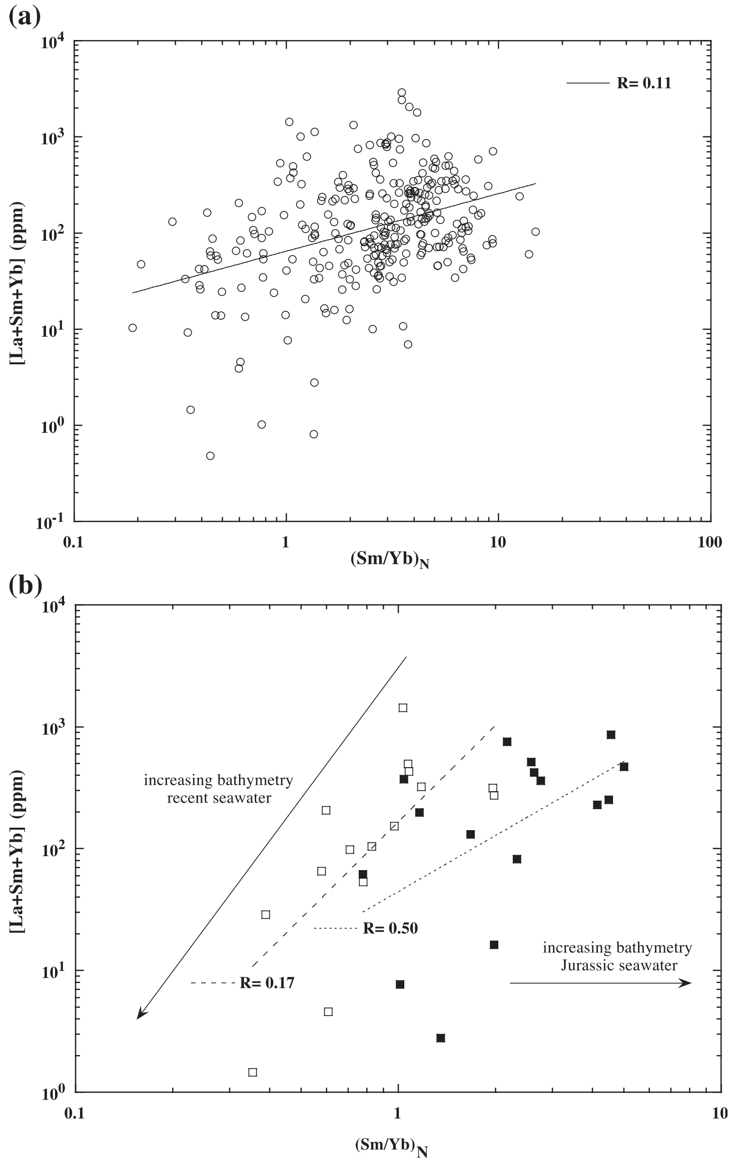

Fig. 6. Variations of sum of the three selected REE (La + Sm + Yb) with $(Sm/Yb)_N$ ratio (data from Table 2). (a) Whole set, note the weak correlation. (b) Subsets from: (1) contemporary fish remains (Elderfield and Pagett, 1986), open squares; (2) Jurassic fish and reptile remains (Picard et al., 2002), filled squares. Note that bathymetry mostly decreases the sum of REE in contemporary oceans with little decrease of the $(Sm/Yb)_N$ ratio, while in Jurassic environments, palaeobathymetry causes a significant increase of the $(Sm/Yb)_N$ ratio and a slight increase of the REE sum. This more likely reflects a change in REE scavenging in oceans prior to 110 Ma and after 80 Ma than a change in the REE uptake mechanism in biogenic apatites.

composition and rare earth element distribution in early Paleozoic biogenic apatite from Baltoscandia: a signature of Iapetus ocean water. Geology 26, 1083–1086.

Fowler, S.W., Buat-Menard, P., Yokoyama, Y., Ballestra, S., Holm, E., Van Nguyen, H., 1987. Rapid removal of Chernobyl fallout from Mediterranean surface waters by biological activity. Nature 329, 56–58.

Frakes, L.A., 1999. Estimating the global thermal state from Cretaceous sea surface and continental temperature data. In: Barrera, E., Johnson, C.C. (Eds.), Evolution of the Creta-

ceous Ocean–Climate System. Spec. Pap.-Geol. Soc. Am., pp. 49–57.
Girard, C., Lécuyer, C., 2002. Variations in Ce anomalies of conodonts through the Frasnian/Famennian boundary of Poland (Kowala–Holy Cross Mountains): implications for the redox state of seawater and biodiversity. Palaeogeogr. Palaeoclimatol. Palaeocol. 181, 299–311.
Grandjean, P., 1989. Les terres rares et la composition isotopique du néodyme dans les phosphates biogènes: traceurs des processus paléo-océanographiques et sédimentaires. PhD Thesis, I.N.P.L. Nancy, France. 319 pp.
Grandjean, P., Albarède, F., 1989. Rare earth elements in old biogenic apatites. Geochim. Cosmochim. Acta 57, 2507–2514.
Grandjean, P., Cappetta, H., Michard, A., Albarède, F., 1987. The assessment of REE patterns and $^{143}Nd/^{144}Nd$ ratios in fish remains. Earth Planet. Sci. Lett. 84, 181–196.
Grandjean, P., Cappetta, H., Albarède, F., 1988. The REE and ε_{Nd} of 40–70 Ma old fish debris from the West-African platform. Geophys. Res. Lett. 15, 389–392.
Grandjean-Lécuyer, P., Feist, R., Albarede, F., 1993. Rare earth elements in old biogenic apatites. Geochim. Cosmochim. Acta 57, 2507–2514.
Gromet, L.P., Dymek, R.F., Haskin, L.A., Korotev, R.L., 1984. The North American Shale composite: its compilation, major and trace element characteristics. Geochim. Cosmochim. Acta 48, 2469–2482.
Huber, B.T., Hodell, D.A., Hamilton, C.P., 1995. Middle–Late Cretaceous climate of the southern high latitudes: stable isotopic evidence for minimal equator-to-pole thermal gradients. Geol. Soc. Amer. Bull. 107, 1164–1191.
Kemp, R.A., Trueman, C., 2003. Rare earth elements in Solnhofen biogenic apatite: geochemical clues to the paleoenvironment. Sediment. Geol. 155, 109–127.
Koeppenkastrop, D., De Carlo, E.H., 1992. Sorption of rare earth elements from seawater onto synthetic mineral particles: an experimental approach. Chem. Geol. 95, 251–263.
Koeppenkastrop, D., De Carlo, E.H., Roth, M., 1991. A method to investigate the interaction of rare earth elements in aqueous solution with metal oxides. J. Radioanal. Nucl. Chem. 152, 337–346.
Kolodny, Y., Raab, M., 1988. Oxygen isotopes in phosphatic fish remains from Israel: paleothermometry of tropical Cretaceous and Tertiary shelf waters. Palaeogeogr. Palaeoclimatol. Palaeoecol. 64, 59–67.
Lécuyer, C., Grandjean, P., O'Neil, J.R., Cappetta, H., Martineau, F., 1993. Thermal excursions in the ocean at the Cretaceous–Tertiary boundary (northern Morocco): the $\delta^{18}O$ record of phosphatic fish debris. Palaeogeogr. Palaeoclimatol. Palaeoecol. 105, 235–243.
Lécuyer, C., Grandjean, P., Barrat, J.A., Emig, C.C., Nolvak, J., Paris, F., Robardet, M., 1998. $\delta^{18}O$ and REE contents of phosphatic brachiopods: a comparison between modern and lower Paleozoic populations. Geochim. Cosmochim. Acta 62, 2429–2436.
Lécuyer, C., Bogey, C., Garcia, J.-P., Grandjean, P., Barrat, J.-A., Floquet, M., Bardet, N., Pereda-Superbiola, X., 2002. Stable isotope compositions and rare earth element content of vertebrate remains from the late Cretaceous of northern Spain (Laño): did the environmental record survive? Palaeogeogr. Palaeoclimatol. Palaeoecol. 193, 457–471.
Liu, Y.-G., Miah, M.R.U., Schmitt, R.A., 1988. Cerium: a chemical tracer for paleo-oceanic redox conditions. Geochim. Cosmochim. Acta 52, 1361–1371.
Picard, S., Garcia, J.P., Lécuyer, C., Sheppard, S.M.F., Cappetta, H., Emig, C., 1998. $\delta^{18}O$ values of coexisting brachiopods and fish: temperature differences and estimates of paleo-water depths. Geology 26, 975–978.
Picard, S., Lécuyer, C., Barrat, J.-A., Garcia, J.-P., Dromart, G., Sheppard, S.M.F., 2002. Rare earth element contents of Jurassic fish and reptile teeth and their potential relation to seawater composition (Anglo-Paris Basin, France and England). Chem. Geol. 186, 1–16.
Piper, D.Z., 1974. Rare earth elements in the sedimentary cycle: a summary. Chem. Geol. 14, 285–304.
Poulsen, C.J., Barron, E.J., Arthur, M.A., Peterson, W.H., 2001. Response of the mid-Cretaceous global oceanic circulation to tectonic and CO_2 forcings. Paleoceanography 16, 576–592.
Pucéat, E., Lécuyer, C., Sheppard, S.M.F., Dromart, G., Reboulet, S., Grandjean, P., 2003. Thermal evolution of Cretaceous Tethyan marine waters inferred from oxygen isotope composition of fish tooth enamels. Paleoceanography 18, 1029 (doi: 10.1029/2002PA000823).
Reynard, B., Lécuyer, C., Grandjean, P., 1999. Crystal-chemical controls on rare-earth element concentrations in fossil biogenic apatites and implications for paleoenvironmental reconstructions. Chem. Geol. 155, 233–241.
Roth, P.H., 1986. Mesozoic palaeoceanography of the North Atlantic and Tethys Oceans. In: Summerhayes, C.P., Shackleton, N.J. (Eds.), North Atlantic Palaeoceanography. Spec. Publ.-Geol. Soc., pp. 299–320.
Saito, T., Van Donk, J., 1974. Oxygen and carbon isotope measurements of late cretaceous and early tertiary foraminifera. Micropaleontology 20, 152–177.
Scotese, C.R., Gahagan, L.M., Larson, R.L., 1988. Plate tectonic reconstructions of the cretaceous and cenozoic ocean basins. Tectonophysics 155, 27–48.
Shields, G., Stille, P., 2001. Diagenetic constraints on the use of Ce anomalies as paleoseawater redox proxies: an isotopic and REE study of Cambrian phosphorites. Chem. Geol. 175, 29–48.
Stille, P., Steinmann, M., Riggs, S.R., 1996. Nd isotopic evidence for the evolution of paleocurrents in the Atlantic and Tethys Oceans during the past 180 Ma. Earth Planet. Sci. Lett. 144, 9–19.
Tappan, H., Loeblich, A.R., 1973. Evolution of the oceanic plankton. Earth Sci. Rev. 9, 207–240.
Wright, J., Seymour, R.S., Shaw, H.F., 1984. REE and Nd isotopes in conodont apatite: variations with geological age and depositional environment. In: Clarck, D.L. (Ed.), Conodont Biofacies and Provincialism. Spec. Pap.-Geol. Soc. Am., vol. 196, pp. 325–340.
Wright, J., Schrarder, H., Holser, W.T., 1987. Paleoredox variations in ancient oceans recorded by rare earth elements in fossil apatite. Geochim. Cosmochim. Acta 51, 631–644.